TIMESTEP SELECTION DURING STREAMLINE SIMULATION VIA TRANSVERSE FLUX CORRECTION

A Thesis

by

ICHIRO OSAKO

Submitted to the Office of Graduate Studies of
Texas A&M University
in partial fulfillment of the requirements for the degree of

MASTER OF SCIENCE

December 2003

Major Subject: Petroleum Engineering

TIMESTEP SELECTION DURING STREAMLINE SIMULATION

VIA TRANSVERSE FLUX CORRECTION

A Thesis

by

ICHIRO OSAKO

Submitted to the Office of Graduate Studies of
Texas A&M University
in partial fulfillment of the requirements for the degree of

MASTER OF SCIENCE

Approved as to style and content by:

Akhil Datta-Gupta (Chair of Committee)	Yalchin Efendiev (Member)
Hans C. Juvkam-Wold (Member)	Hans C. Juvkam-Wold (Head of Department)

December 2003

Major Subject: Petroleum Engineering

ABSTRACT

Timestep Selection During Streamline Simulation via Transverse Flux Correction.

(December 2003)

Ichiro Osako, B.Eng., Waseda University, Japan

Chair of Advisory Committee: Dr. Akhil Datta-Gupta

Streamline simulators have received increased attention because of their ability to effectively handle multimillion cell detailed geologic models and large simulation models. The efficiency of streamline simulation has relied primarily on their ability to take large timesteps with fewer pressure solutions within an IMPES formulation. However, unlike conventional finite-difference simulators, no clear guidelines are currently available for the choice of timestep for pressure and velocity updates. That is why we need largely an uncontrolled approximation, either managed by engineering judgment or by potentially time-consuming timestep size sensitivity studies early in a project. This will clearly lead us to the lack of understanding of numerical stability and error estimates during the solution.

This research presents a novel approach for timestep selection during streamline simulation that is based on three elements. First, we reformulate the equations to be solved by a streamline simulator to include all of the three-dimensional flux terms – both aligned with and transverse to the flow directions. These transverse flux terms are totally neglected within the existing streamline simulation formulations. Second, we propose a simple grid-based corrector algorithm to update the saturation to account for the transverse flux. Third, we provide a discrete CFL (Courant-Friedrich-Levy) formulation for the corrector step that leads to a mechanism to ensure numerical stability via the choice of a stable timestep for pressure updates. This discrete CFL formulation now

provides us with the same tools for timestep control as are available within conventional reservoir simulators.

We demonstrate the validity and utility of our approach using a series of numerical experiments in homogeneous and heterogeneous ¼ five-spot patterns at various mobility ratios. For these numerical experiments, we pay particular attention to favorable mobility ratio displacements, as they are known to be challenging to streamline simulation. Our results clearly demonstrate the impact of the transverse flux correction on the accuracy of the solution and on the appropriate choice of timestep, across a range of mobility ratios. The proposed approach eliminates much of the subjectivity associated with streamline simulation, and provides a basis for automatic control of pressure timestep within full field streamline applications.

DEDICATION

This thesis is dedicated to my family in Japan, especially to my parents, Hitoshi and Yoko, and my brother, Takuro, and grandmother, Chiyoko for their love, care and encouragement.

ACKNOWLEDGMENTS

I would like to take this opportunity to express my deepest gratitude and appreciation to my advisor and committee chair, Dr. Akhil Datta-Gupta, for his continuous encouragement, and especially for his academic guidance. And also I would like to extend my sincere thanks to Dr. Hans C. Juvkam-Wold and Dr. Yalchin Efendiev for serving as committee members.

I would like to acknowledge Dr. Michael J. King in EPTG, BP America, Inc for his academic guidance and the helpful discussion.

I would like to acknowledge ChevronTexaco Exploration & Production Technology Company for providing me many experiences and the opportunity to apply my technical knowledge during my summer internship. I would like to thank my mentors: Manoj Choudhary, Steve Johnson in ChevronTexaco EPTC, and Dr. Neil Barman, and Dr. Seongsik Yoon in Seismic Micro-Technology.

I would like to thank all members of Dr.Arihara's research group in Waseda University. Especially for Dr. Norio Arihara and Sutopo-hakase (now with Institut Teknologi Bandung), and my cute girl friend, Sato-chan, for their continuous encouragement from Japan.

Finally I want to thank my friends in the reservoir characterization group, Dr. Arun Kharghoria (now with PetroTel), Dr. Sangheon Lee (now with ChevronTexaco), Dr. Zhong He, Harshal Parikh (now with Intera), Hector Perez (now with Ecopetrol), Ahmed Al-Hutheli (now with Saudi Aramco), Ahmed Daoud, Hao Cheng, Il Nam, Eduardo Jimenez, Dayo Oyerinde, Mishal Al-Harbi, Chengwu Yuan, and Leonardo Vega, for giving me a great memories during my graduate study at Texas A&M University. The facilities and resources provided by the Harold Vance Department of Petroleum Engineering of Texas A&M University are gratefully acknowledged.

TABLE OF CONTENTS

Page

LIST OF FIGURES

FIGURE Page

FIGURE Page

FIGURE Page

LIST OF TABLES

CHAPTER I

INTRODUCTION

Compared to conventional finite difference simulation, 3-D streamline simulation has moved from a research topic to a commercial product rather recently. Finite difference simulation made this transition in the 1960's while commercial streamline simulators have only been available since the 1990's.[1] Technically, the oil industry literature on streamtubes dates back to the 1930's, but the three-dimensional streamline approaches are much more recent.[2-8] Many of the features that we take for granted in finite difference simulation are still missing from streamline approaches.

Our work attempts to resolve one such gap. That is an analysis of the numerical stability of the streamline formulation, a pre-requisite to the choice of a stable timestep for pressure updates during streamline simulation. The stability analysis is based upon a discrete CFL formulation. It provides us with the same tools for timestep control as are available within conventional reservoir simulators. We expect that this formulation will allow streamline simulators to provide as robust answers as we take for granted with finite difference calculations, while retaining the speed and performance characteristics that make streamline simulators of value today.

Besides numerical stability, also external factors such as reservoir development and management will control the timestep size in a flow simulator.[7] As we develop and manage a field we are introducing new wells, and changing our well rates, potentially on a daily basis. If these changes in boundary conditions are significant, then the timestep size for our flow simulation must honor them. Of course, when screening geologic models, or when developing long-term depletion plans for reservoirs, the frequency of

---

This Thesis follows the style of *Society of Petroleum Engineers Journal*.

reservoir management activities may not be a severe limitation. In that case, timestep size is then primarily controlled by the requirement for numerical stability.

A numerical stability analysis for streamline simulation is the primary focus of this study. The development we supply will also explain the ability of streamline simulators to take large timesteps. The results are in complete agreement with our physical intuition, and justify much of the current industry practice. However, it will also show us when timesteps for pressure updates are too large. Paradoxically, favorable mobility ratio waterflood, one of the most common secondary recovery processes, turns out to be a difficult calculation for streamline simulators. Calculations of unstable displacements and miscible viscous fingering are much easier in comparison. As we continue to advance the breadth and complexity of mechanisms that are included within a streamline simulator, for example, compositional processes, the requirement for a stability analysis and the choice of appropriate timestep clearly becomes of paramount importance.

1.1 Streamline Simulation

The streamline simulation has been used widely for the petroleum industry for the recent decade. The computational expense as well as the accuracy will be considered for selecting the reservoir simulation. In that point, the streamline simulation has the significant advantage that can calculate much faster than conventional finite-difference simulators. The advantage will also make it possible to handle millions cells that represent complex geological features.

Based on the IMPES (IMplicit-Pressure-Explicit-Saturation) method, we solve for the pressure first in each grid block and trace streamlines respected with the calculated block pressure. At the same time, we will calculate the particle transit time within each grid block the streamline breaks through. The transit time is so called Time of Flight[2] and becomes the coordinate for the saturation updating. Once we get Time of

Flight, we can map grid block properties such as the water saturation and pressure on the streamline. It will allow us to change the 3-D grid block coordinate to the pseudo 1-D Time of Flight coordinate and make the calculation for updating the saturation much faster than conventional finite-difference simulation.

The streamline simulation has some disadvantages behind the big advantage. First, Time of Flight is defined on a fixed set of streamlines that is simply the steady state approximation. Second, unsteady states will vary streamlines during the certain timestep for the pressure update and it will generate transverse fluxes. Third the quality of the IMPES approximation will depend on the magnitude of the transverse flux between pressure updates, but we don't have any ways to take into account for that. Therefore we need a consideration of the accurate timestep analysis under the unsteady state conditions.

1.2 Transverse Flux

Streamline is a pathline of a particle which has the certain amount of fluid. The trajectory of streamline uses three dimensional velocities, V_x, V_y, V_z which are components of the average velocity vector. **Figure 1.1** shows a velocity vector with a definite direction at the specific point in the flow domain which is at any instant of time. Taking instantaneous curves which are always tangent to the velocity vector at one point makes streamline of the flow. Thus the particle containing the certain amount of fluid has always tangent direction to the velocity vector and the flow is called the longitudinal flux. As long as we use streamline, the fluid flow in porous media is assumed to be longitudinal flow and the streamline is not going to move for a period. For steady state condition, the assumption is absolutely right. However for unsteady state condition, it is easy to imagine that the instantaneous curve is going to change because of that and the movement of fluid is not only tangent to the average velocity vector. In such case, we need to take into account for the flow other than the longitudinal flux in streamline simulation.

The transverse flux is a flow between streamlines because of the compressibility and diffusivity of the fluid flow. We can imagine those fluxes as the leaking fluid from streamlines. Under the unsteady state condition such as incompressible flow, the presences of gravity and capillary pressure effects, the average velocity vector do not move simply the same as the phase velocity vector. That will move streamlines and generate transverse flux. However we can take into account for gravity segregations[4] and capillary effects[9] using an operator splitting method recently, the transverse flux because of incompressible flow has not been solved well.

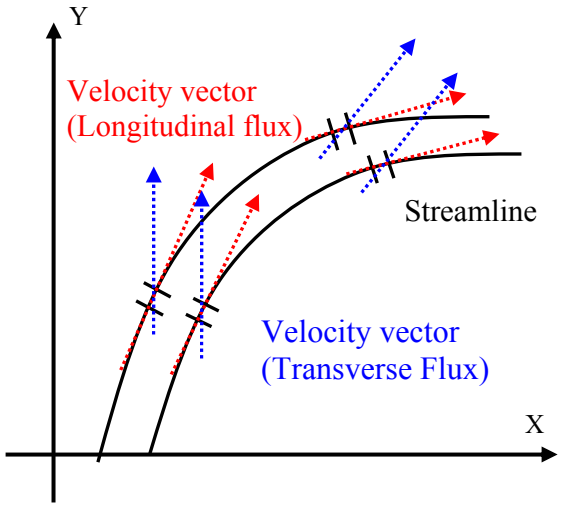

Figure 1.1 – Streamline and velocity vector

1.3 CFL (Courant-Friedrich-Levy) Number

In conventional simulators the pressure and saturation will be solved on the grid block coordinate. Therefore they do not have restrictions that streamline simulation has, and which make it possible to handle the effects of compressible and diffusive flows in conventional simulators. On the other hand they have a timestep restriction for stability requirement because of using the grid block coordinate, while streamline simulation

does not be required under the assumption of incompressibility that allows us to solve the saturation evolution equation on the streamline. In this work we focus on how to select the optimum timestep for the pressure update that assures the streamlines are stable and generate no transverse fluxes during the time. For the challenge we will use CFL (Courant-Friedrich-Levy) [10] number. CFL number is well known as the numerical stability requirement for the explicit finite-difference method that is a simple interpretation for this stability requirement. The fastest wave must not pass across an entire cell during a timestep or simply all flux coming into an entire cell during a timestep must be lower than the pore volume of the cell. Its use is to understand the numerical stability and the timestep size requirements for its usual IMPES solution. For streamline simulation the CFL construction is identical, except now the correction velocity replaces the total velocity.

1.4 Objectives of the Study

The main objective of this research is to provide a novel approach for timestep selection in streamline simulation based on the stability analysis using a discrete CFL formulation. Followings are the basic objectives:

- Provide a new formulation to quantify the errors introduced by the neglect of transverse flux.
- Introduce a discrete CFL number based on the transverse flux and demonstrates its ability to provide the effective timestep control for streamline simulation.
- Compute numerical accuracy using a discrete CFL and the saturation corrections introduced by the inclusion of transverse flux in our formulation.

1.5 Methodology

We begin with a discussion of the streamline time of flight formulation as it provides us with a clear means of distinguishing between longitudinal and transverse flux. We then move to the discussion of the transverse flux, and of unsteady state effects in general

during streamline simulation. Specifically, we provide a new formulation to quantify the errors introduced by the neglect of transverse flux. We also introduce a discrete CFL number based on the transverse flux and demonstrate its ability to provide an effective timestep control for streamline simulation. Finally, we return to questions of numerical accuracy, and the saturation corrections introduced by the inclusion of transverse flux in our formulation. Our proposed new formulation, the application of the discrete CFL number, and the discussion of numerical accuracy, provide the bulk of the thesis. We have chosen to work with simple 2D waterflood models (homogeneous and heterogeneous ¼ five-spot patterns with quadratic relative permeabilities, at various mobility ratios) to clearly demonstrate the stability mechanisms as a synthetic case.

1.6 Chapter Organization

Four chapters will organize this thesis. Chapter I is an introduction and describes the general ideas of the streamline simulation, the transverse flux and the CFL number. Chapter II will show theoretical aspects; a new formulation to quantify the errors introduced by the neglect of transverse flux, the saturation corrections introduced by the inclusion of transverse flux in our formulation, and finally a discrete CFL number based on the transverse flux which gives us the selection of optimal timesteps in streamline simulations. Chapter III will show results of some synthetic examples. We will demonstrate the validity of a new formulation and its ability to provide an effective timestep control for streamline simulation. Finally Chapter IV provides discussions conclusions and future work from this work.

CHAPTER II
THEORETICAL BACKGROUND

Selection of timestep in reservoir simulations is a top priority not only to estimate accurate reservoir performance but also to obtain cost effective development strategies in actual field studies. Timestep selection of conventional simulators is conducted using the criteria based on the maximum expected change of saturation or pressure, material balance error, and CFL numbers and so on, however those methods are only applied to grid block based calculation such as finite-difference schemes.

The selected timestep based on the criteria such as the maximum change of primary unknown variables in reservoir simulation, material balance error, and CFL numbers will be calculated only on each grid block not for along streamlines. Only way for selection of timestep in streamline simulation is either time-consuming trial error sensitivity studies or managed by engineering judgment. This will create some potentials to have a large uncertainty and miss leading for future performances from the beginning of the development stage in field studies. It is therefore evident that the timestep selection criteria for streamline simulation is very important and it gives clear guideline for the most optimal and cost effective reservoir studies and error estimates from the simulations.

2.1 Streamline Time of Flight Formulation

The streamline time of flight formulation is the means whereby the two-dimensional streamtube simulation approaches have been extended to three dimensions.[2,3,10,11] Rather than performing volumetric calculations based upon streamtubes, we can think of streamlines running along the center of each streamtube. Instead of deriving fluid velocities from flux conservation and the explicit geometry of the tubes, we can explicitly calculate velocities and time of flight along the lines, and make the tube

geometries implicit. Once the geometry is made implicit, there is little difference between two-dimensional and three-dimensional calculations. In fact, the solution now simply consists of a sum of one-dimensional calculations along streamlines. Whether we then use analytic or numerical approaches to solve our saturation evolution equations, these one-dimensional problems can be solved extremely rapidly and hence the effectiveness of the streamline simulators.

Formally, how do we derive this approach? Let's start with the simplest possible set of equations, those for two-phase incompressible waterflood. Neglecting source and sink terms, we have one equation for the saturation evolution, and another that expresses the conservation of volume (oil plus water).[12-13]

$$\phi \frac{\partial S_w}{\partial t} + \nabla \bullet \left(\vec{u} \, f_w \right) = 0 \tag{2.1}$$

$$\nabla \bullet \vec{u} = 0 \tag{2.2}$$

The total fluid Darcy velocity is aligned with the local pressure gradient.

$$\vec{u} = -\lambda_t \nabla P \tag{2.3}$$

The coefficient between $\vec{u}$ and ∇P is the total mobility, which depends upon the permeability of the medium, and the relative permeabilities and viscosities of the fluid phases.

$$\lambda_t = k \cdot \left(\frac{k_{rw}}{\mu_w} + \frac{k_{ro}}{\mu_o} \right) \tag{2.4}$$

The fractional flow of water is equal to the ratio of water phase and total mobilities.

$$f_w = \left(\frac{k_{rw}}{\mu_w} \right) \Big/ \left(\frac{k_{rw}}{\mu_w} + \frac{k_{ro}}{\mu_o} \right) \tag{2.5}$$

For most systems, the permeability depends upon position, $k(\vec{x})$, whilst the relative permeabilities depend upon the phase saturation. Let's now introduce the time of flight.

Consider a set of waterflood injectors and producers running at steady state, and for now, let's ignore all unsteady state effects induced by the waterflood itself. Streamlines begin at the injectors and run to the producers. Depending upon the voidage replacement ratio, lines may run to and from an aquifer or the reservoir boundaries. In fact, we may apply this formulation even for primary depletion, if we work at a sequence of pseudo steady states;[14] however, we will not discuss this now. On each streamline, introduce a particle that moves with the interstitial velocity, $\vec{u}/\phi$, and then integrate the time it takes for the particle to move from one point to another along the line. In differential form we have:[2,3]

$$\vec{u} \bullet \nabla \tau = \phi \tag{2.6}$$

As each point in space lies on a streamline, we can define τ throughout the domain, $\tau(\vec{x})$. Although this conceptualization invokes a single velocity field and particles, the time of flight formulation is not a particle tracker, nor is it restricted to single-phase flow.[2,3]

The time of flight, τ, has units of time but in fact it will function like a distance. We see this after making a formal spatial coordinate transformation. A three dimensional coordinate transformation requires three spatial coordinates. One is supplied by $\tau(\vec{x})$. The other two are the bi-stream functions, $\psi(\vec{x})$ and $\chi(\vec{x})$, for instance, described by Bear.[15]

$$\vec{u} = \nabla \psi \times \nabla \chi \tag{2.7}$$

As with the Lagrangian stream function in two dimensions, any velocity field described by **Eq.(2.7)** will automatically satisfy volume conservation, **Eq.(2.2)**. We can now generate the formal coordinate transformation from (x,y,z) to (τ,ψ,χ). The properties of

this transformation are described more fully elsewhere.[3] Here we will express the gradient operator in terms of gradients and derivatives in τ, ψ, and χ.

$$\nabla = (\nabla\tau)\frac{\partial}{\partial\tau} + (\nabla\psi)\frac{\partial}{\partial\psi} + (\nabla\chi)\frac{\partial}{\partial\chi} \tag{2.8}$$

Because of the orthogonality implicit in **Eq.(2.8)**, we can now simplify the flux term in **Eq.(2.1)** as follows

$$\nabla \bullet (\vec{u}\, f_w) = (\vec{u} \bullet \nabla) f_w = \phi \frac{\partial f_w}{\partial \tau} \tag{2.9}$$

where we have used the time of flight definition in **Eq.(2.6).** The three dimensional spatial derivative of **Eq.(2.1)** can now be replaced by the single spatial derivative with respect to τ

$$\frac{\partial S_w}{\partial t} + \frac{\partial f_w}{\partial \tau} = 0 \tag{2.10}$$

Streamline simulators may solve what is now a collection of one-dimensional equations using either analytic or numerical techniques. In either case, the 1-D solutions along streamlines are decoupled from the underlying grid for velocity calculations and the solution along each streamline may be optimized separately, providing an extremely rapid numerical calculation. We will not discuss these implementation details at all, as they are not the focus of this paper, and as they are reasonably well documented in the literature.[2-8,14-17]

2.2 Saturation Correction via Transverse Flux and Unsteady State Effects

The elegance of the streamline time of flight formulation is apparent in **Eq.(2.10)**. Unfortunately, so is its fundamental limitation. When we implement the numerical solution along lines for **Eq.(2.10)**, we generally do so as a sequence of steady state approximations, just as we do for an IMPES formulation in a finite difference simulator. For unsteady state flow, the streamlines vary in time generating flux transverse to the flow direction. Streamlines are regenerated periodically via pressure updates and fluid

saturations and concentrations are mapped from the old streamlines to the new streamlines. The quality of the IMPES approximation will naturally depend upon the magnitude of the transverse flux that is unaccounted for between successive pressure updates. There are several questions that remain unanswered here. Physically, is the steady state formulation now a reasonable one? Numerically, is there evidence for loss of stability? Is there an approach we can take that illuminates the issues associated with unsteady state velocities?

One approach is to apply a moving coordinate Lagrangian transformation. If we define τ, ψ, and χ with respect to the instantaneous velocity, then the spatial derivative term of **Eq.(2.1)** retains the simple form of **Eq.(2.10)**. Unfortunately, as τ, ψ, and χ are now all time dependent, the $\frac{\partial S_w}{\partial t}$ term of **Eq.(2.1)** generates three additional terms of the form $\frac{\partial S_w}{\partial \tau}\frac{\partial \tau}{\partial t}$ in the equivalent to **Eq.(2.10)**. This is too complex a formulation.

A simpler approach is to distinguish between the initial and the instantaneous velocities during a time step, and to define τ, ψ, and χ with respect to the initial velocity of the time step. For instance,

$$\vec{u}_0 \bullet \nabla \tau = \phi \tag{2.11}$$

and similarly for ψ and χ. As before, we do not need to determine ψ and χ explicitly, as these coordinates vanish from the differential equations. The spatial derivative term can now be written as its initial approximation, and a correction.

$$\begin{aligned} \vec{u} \bullet \nabla f_w &= \vec{u}_0 \bullet \nabla f_w + (\vec{u} - \vec{u}_0) \bullet \nabla f_w \\ &= \phi \frac{\partial f_w}{\partial \tau} + (\vec{u} - \vec{u}_0) \bullet \nabla f_w \end{aligned} \tag{2.12}$$

The second term in **Eq.(2.12)** represents the transverse flux because of unsteady velocity fields and will clearly vanish for steady state conditions. And, as in much of the

streamline literature, we now apply operator splitting and represent the time derivative as a convective time step followed by what we term a corrector time step:[4,16] $\frac{\partial S_w}{\partial t} \rightarrow \frac{\partial S_w}{\partial t_1} + \frac{\partial S_w}{\partial t_2}$.

Eq.(2.1) now becomes

$$\phi \frac{\partial S_w}{\partial t_1} + \phi \frac{\partial S_w}{\partial t_2} + \phi \frac{\partial f_w}{\partial \tau} + (\vec{u} - \vec{u}_0) \bullet \nabla f_w = 0 \tag{2.13}$$

We may group and split the terms in **Eq.(2.13)** into the following two equations:

$$\frac{\partial S_w}{\partial t_1} + \frac{\partial f_w}{\partial \tau} = 0 \tag{2.14}$$

$$\phi \frac{\partial S_w}{\partial t_2} + (\vec{u} - \vec{u}_0) \bullet \nabla f_w = 0 \tag{2.15}$$

To within the operator splitting approximation, this pair of equations is equivalent to the original three-dimensional flow equation. The first equation, **Eq.(2.14)** is the usual streamline evolution equation. The second equation, **Eq.(2.15)** is of the same form as our usual conservation equation, **Eq.(2.1),** but with the total Darcy velocity replaced by a correction velocity. It includes any and all unsteady state effects, whether transverse or longitudinal. Based on **Eqs.(2.14)** and **(2.15)**, we can now view the streamline simulator simply as a preconditioner to a conventional finite difference simulator. We can solve **Eq.(2.15)** using finite difference methods to update the streamline-derived saturations.

What have we achieved? As an industry, we have a great deal of expertise in solving each of these equations.[13] Now we recognize that rigorous streamline simulation relies on solving these two equations in a coupled fashion. For convection-dominated flow, the first term is the most important, while the second equation supplies the correction. When the changes in velocity are small during a time step, we can expect that current streamline simulators will work well. This certainly is consistent with our physical intuition.

How well does this correction scheme work? First, we need to describe a few implementation details. **Eq.(2.14)** is solved as in any streamline simulator. During each time step of a simulator, saturations are resampled from cells to lines, the saturations are then modified along the lines according to the evolution equation, and then these new saturations are averaged back onto the cells. **Eq.(2.15)** can now be used to correct the grid block saturations.

How large is the saturation correction during the time step? For each cell, we can take the time integral of **Eq.(2.15)**:

$$\begin{aligned}\int_0^{\Delta t} dt\,(\vec{u}-\vec{u}_0)\bullet\nabla f_w &\approx \frac{\Delta t}{2}\left[\left((\vec{u}-\vec{u}_0)\bullet\nabla f_w\right)_{Initial}+\left((\vec{u}-\vec{u}_0)\bullet\nabla f_w\right)_{Final}\right] \\ &= \frac{\Delta t}{2}\left((\vec{u}-\vec{u}_0)\bullet\nabla f_w\right)_{Final}\end{aligned} \tag{2.16}$$

All terms in **Eq.(2.16)** are known except the final velocity. Even this will be calculated at the beginning of the next time step. As this correction is cell based, it is, in fact, more convenient to take the equations back to conservation form when calculating the saturation correction.

$$\begin{aligned}\iiint_{\Delta x\,\Delta y\,\Delta z} dV\,(\vec{u}-\vec{u}_0)\bullet\nabla f_w &= \iiint_{\Delta x\,\Delta y\,\Delta z} dV\,\nabla\bullet\left((\vec{u}-\vec{u}_0)f_w\right) \\ &= \oiint_A da\,(\vec{u}-\vec{u}_0)\bullet\hat{n}f_w\end{aligned} \tag{2.17}$$

2.3 Timestep Selection Using Correction CFL Number

One of the objectives in this study is to select an optimal timestep for streamline simulation. Since we are able to quantify unsteady state effect during the certain timesptep using **Eq.(2.15)**, we provide a discrete CFL formulation for the corrector step that leads to a mechanism to ensure numerical stability via the choice of a stable time step for pressure updates. This discrete CFL formulation now provides us with the same

tools for time step control as are available within conventional reservoir simulators. What is missing from the conventional CFL formulation?

The CFL construction for one-dimensional Buckley-Leverett waterflood is well known.[18]

$$CFL = \frac{u}{\phi}\frac{\Delta t}{\Delta x} f_w' \tag{2.18}$$

The IMPES CFL stability requirement is $CFL \le 1$. There is a simple interpretation for this stability requirement. The fastest wave must not pass across an entire cell during a time step. The interstitial fluid speed is u/ϕ and Δx is the distance to be covered. The factor of f_w' is the Buckley-Leverett speed of the saturation S_w.

How should we extend the CFL construction to three dimensions? In fact, a solution exists in the literature,[18, 19]

$$CFL = \frac{\Delta t}{\phi}\left(\frac{u_x}{\Delta x} + \frac{u_y}{\Delta y} + \frac{u_z}{\Delta z}\right) f_w' \tag{2.19}$$

where the velocities and saturations are evaluated for each cell. We instead reference the construction to the cell faces, each with their own fluxes and saturation contrasts. Working with cell volumes and volumetric flux instead of distances and velocities, we construct the following discrete CFL number,

$$CFL = \frac{\Delta t}{PV}\sum_{Inflow\ Faces}\left(\vec{u}_f \bullet \vec{n}_f \cdot \underset{S_{wf}}{Max}\left(\frac{[f_w]}{[S_w]}\right)\right) \tag{2.20}$$

The summation is only taken over the inflow faces, e.g., $\vec{n}_f$ is inwardly directed cell face area, and $\vec{u}_f \bullet \vec{n}_f$ must be positive. This is consistent with the interpretation of the CFL number as being dependent upon the fastest wave that moves across a cell.

The only subtlety in this equation is in the discrete form of the wave speed. We can think of the saturation of the adjacent cell, $S_{w,Face}$, flooding into the cell, $S_{w,Cell}$, which will form a Buckley-Leverett profile. Whether we have a pure rarefaction, a shock, or a contact discontinuity depends upon the specific saturations and the fractional flow function. The wave speed that contributes to the CFL restriction is the fastest wave. Specifically, if we consider all saturations S_w intermediate between $S_{w,Face}$ and $S_{w,Cell}$, then the speed is the maximum of $\frac{f_w(S_w) - f_w(S_{w,Cell})}{S_w - S_{w,Cell}}$. If there is no saturation contrast across a face, then this wave speed is set to zero, since there is no contribution to the evolution equation. This form of the discrete CFL number fully accounts for both saturation discontinuities and flow direction reversals.

Eq.(2.20) is the CFL construction for **Eq.(2.1)**. Its use is to understand the numerical stability and the time step size requirements for its usual IMPES solution. For streamline simulation[20], **Eq.(2.15)**, the CFL construction is identical, except now the correction velocity replaces the total velocity, $\vec{u} \to (\vec{u} - \vec{u}_0)$ as shown below,

$$CFL = \frac{\Delta t}{PV} \sum_{Inflow\ Faces} \left((\vec{u}_f - \vec{u}_0) \bullet \vec{n}_f \cdot \underset{S_{wf}}{Max} \left(\frac{[f_w]}{[S_w]} \right) \right) \tag{2.21}$$

At this stage, it is important to distinguish this CFL requirement for the saturation correction step from the CFL requirement for saturation calculation along streamlines. **Eq.(2.14)**, has its own CFL requirement as it is generally solved by conventional one-dimensional finite difference techniques. It is the saturation correction step that limits the pressure time step size.

CHAPTER III

RESULTS AND DISCUSSION

We demonstrate the validity and utility of our approach using a series of numerical experiments in homogeneous and heterogeneous ¼ five-spot patterns at various mobility ratios.

Homogeneous model has 41x41 mesh size, constant permeability value of 8.12mD, and porosity value of 0.03. In **Figure 3.1** we show the ¼ five-spot pattern and the permeability field used for the heterogeneous models. The mesh size is also 41x41. The heterogeneity field is not too extreme, with a minimum value of permeability of 25mD, and a maximum of close to 300mD.

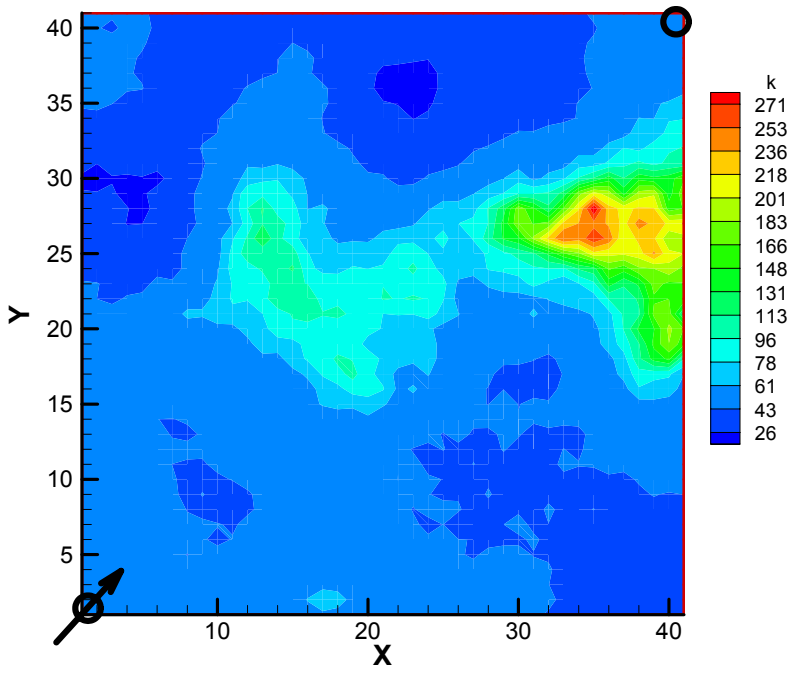

Figure 3.1 – Permeability distribution for heterogeneous case.

3.1 Water Cut Response Analysis

Figure 3.2 to 3.5 is a summary of 4 cases, each showing the water cut from 4 simulation runs for a homogeneous permeability field. These 4 cases correspond to four mobility ratios, M = 0.2, 0.5, 0.9 and 10. The corresponding results for the heterogeneous permeability field are shown in **Figure 3.6 to 3.9**. Quadratic relative permeabilities are used; M is the end-point mobility ratio.

$$k_{ro} = \left(\frac{1 - S_{orw} - S_w}{1 - S_{orw} - S_{wirr}} \right)^2 \tag{3.1}$$

$$k_{rw} = M \frac{\mu_w}{\mu_o} \left(\frac{S_w - S_{wirr}}{1 - S_{orw} - S_{wirr}} \right)^2 \tag{3.2}$$

Of the four simulation runs, one is from Eclipse, which provides a reference solution.[21] The three streamline runs in each plot are calculated with 10, 20, and 60 day time steps for the pressure solution. Each time step is split into convection and the correction steps, **Eq.(2.14)** and **Eq.(2.15)**.

How good are the results of this saturation correction? Unfortunately, the answer is "not very." For the homogeneous permeability field, **Figure 3.2 to Figure 3.5**, as the mobility ratio decreases, generating a more and more favorable waterflood, all but the smallest time step streamline results become inaccurate. For the heterogeneous case, **Figure 3.6 to Figure 3.9**, the same conclusion holds, but with even less validity than for the homogeneous case. We see that even the 10 day simulation results are inaccurate for the most favorable mobility ratio waterflood. Physically we expect that **Eq.(2.15)** will represent the viscous cross-flow across streamlines during a favorable mobility ratio waterflood. This has not happened, or more precisely, the corrections have not been sufficient to provide an accurate solution. What has gone wrong?

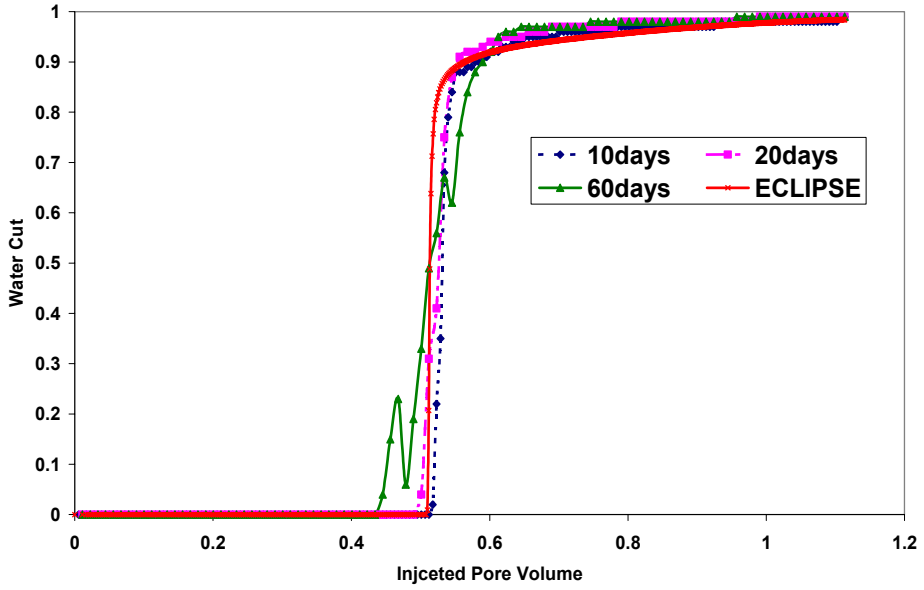

Figure 3.2 – Water cut response for several timesteps: M=0.2 homogeneous case.

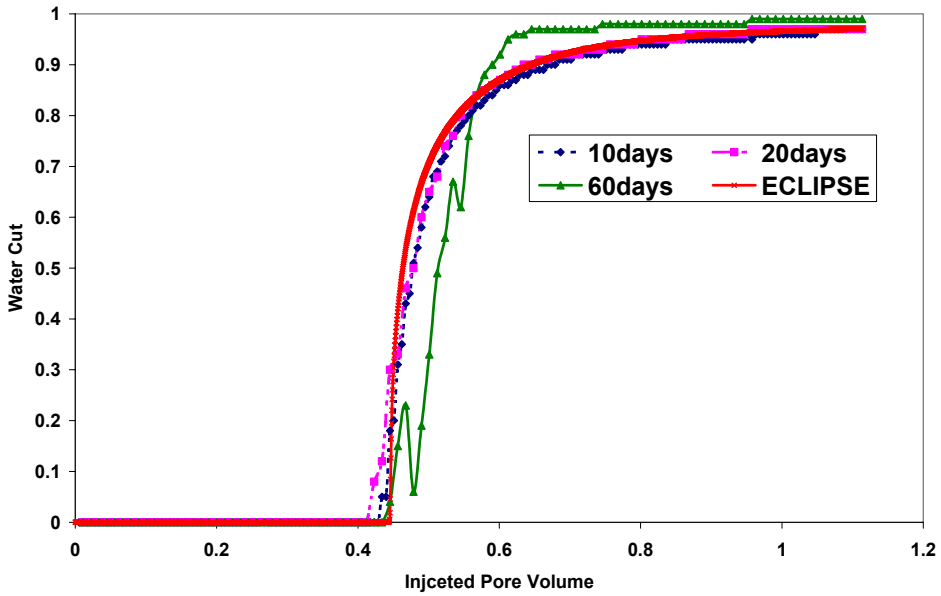

Figure 3.3 – Water cut response for several timesteps: M=0.5 homogeneous case.

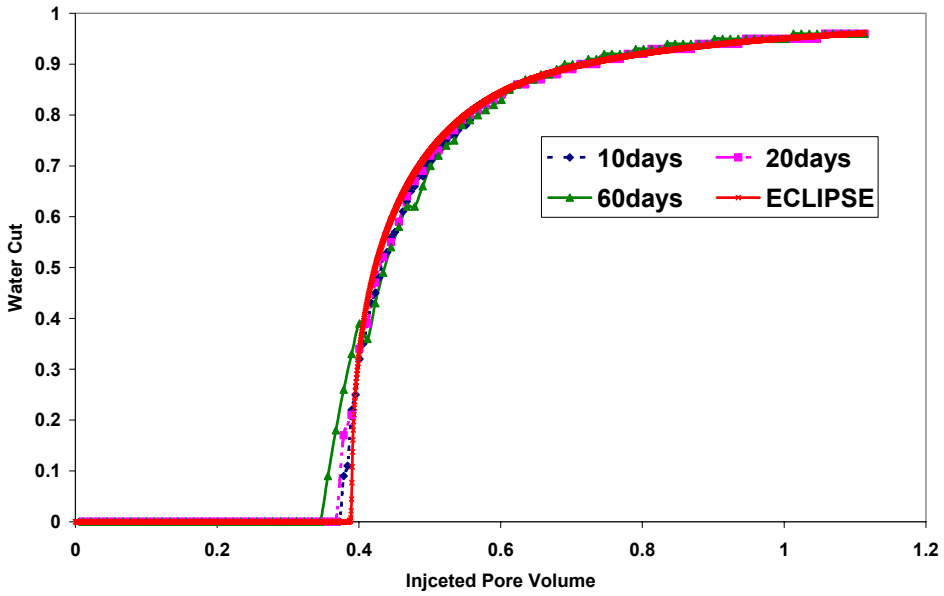

Figure 3.4 – Water cut response for several timesteps: M=0.9 homogeneous case.

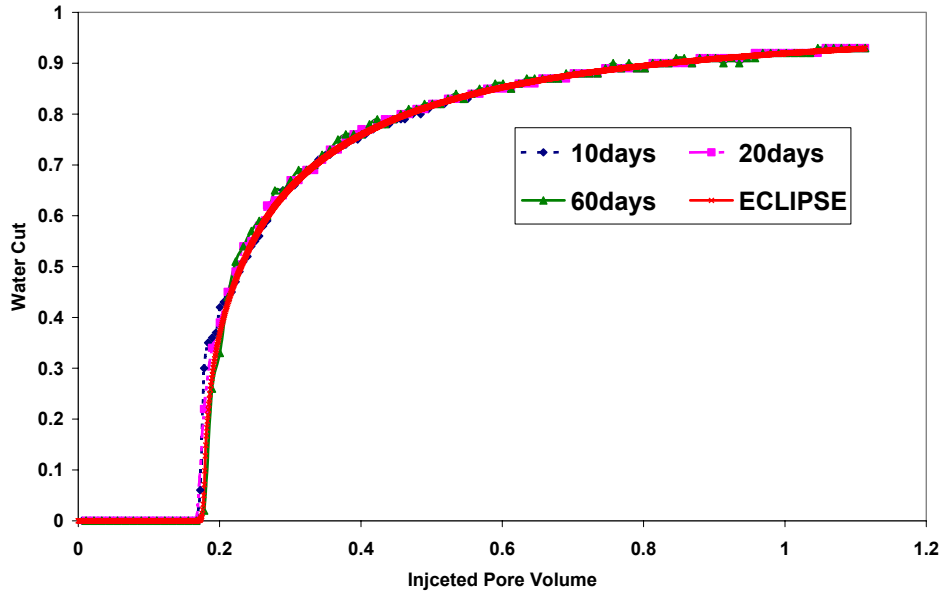

Figure 3.5 – Water cut response for several timesteps: M=10 homogeneous case.

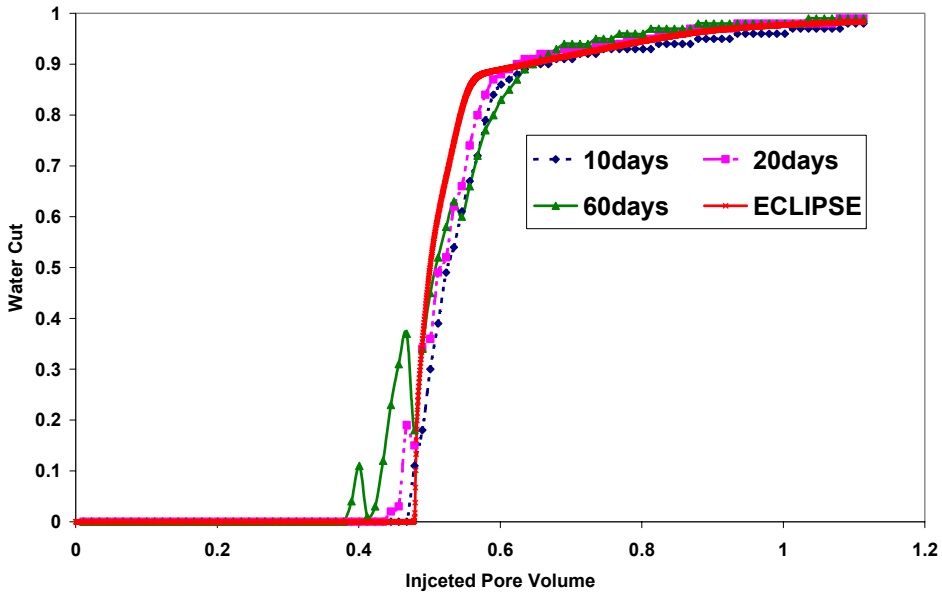

Figure 3.6 – Water cut response for several timesteps: M=0.2 heterogeneous case.

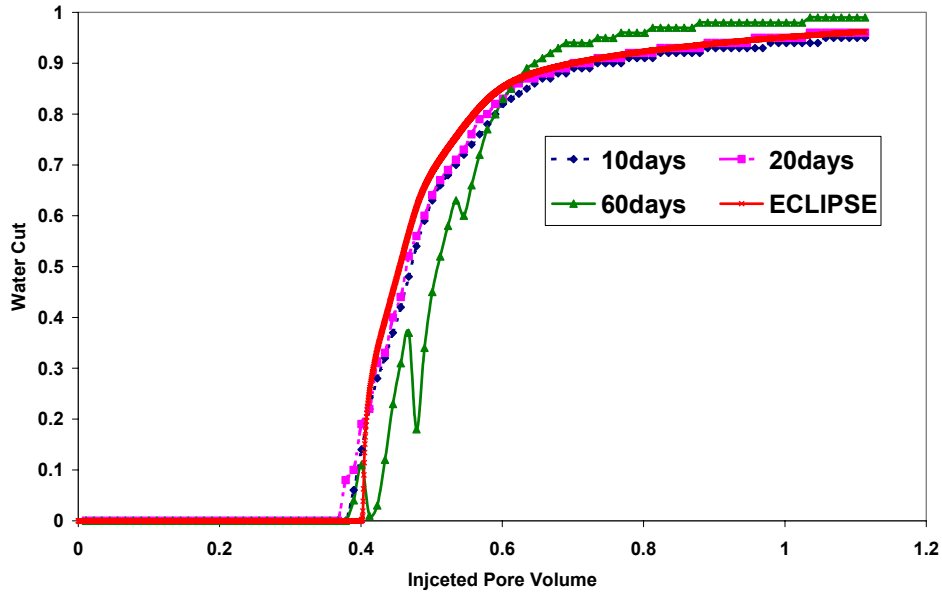

Figure 3.7 – Water cut response for several timesteps: M=0.5 heterogeneous case.

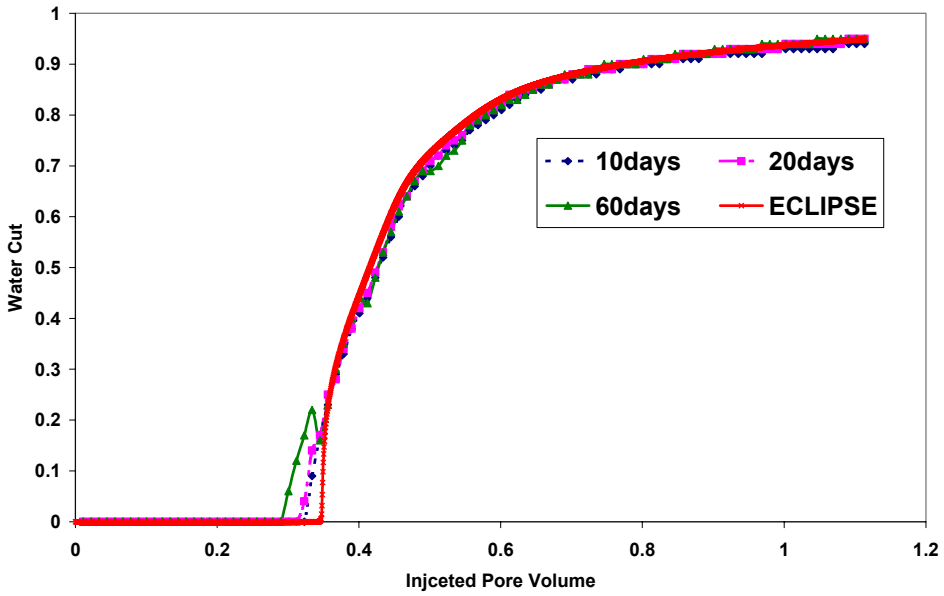

Figure 3.8 – Water cut response for several timesteps: M=0.9 heterogeneous case.

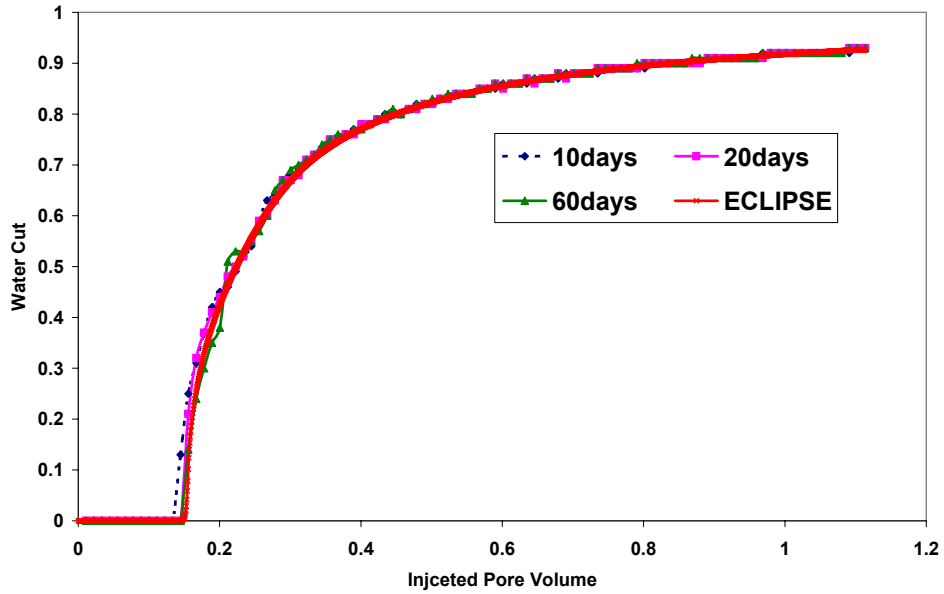

Figure 3.9 – Water cut response for several timesteps: M=10 heterogeneous case.

3.2 CFL Stability Analysis

What is missing from the above analysis? Perhaps the first hint comes from the oscillatory nature of the errors in the water cut plots. The second hint is that the errors increase as either the time step size or as the difference $(\vec{u}-\vec{u}_0)$ increases. The latter increase is most significant for the favorable mobility ratios. Are we violating a CFL stability requirement? Let us now examine the CFL and correction CFL numbers for the same cases. In **Figure 3.10** and **3.11**, we display the CFL numbers after the first time step for the homogeneous permeability field for M = 0.2. In **Figure 3.10** we have shown the discrete CFL number whereas **Figure 3.11** displays the correction CFL number. Each Figure consists of the areal plots of CFL for time step sizes of 10, 20, and 60 days. The legend for each Figure includes information on the maximum CFL number in that Figure. The corresponding Figure for M = 10 are shown in **Figures 3.12** and **3.13**. We have also examined the results for the two additional cases, M = 0.5 and 0.9. For the heterogeneous permeability field, the discrete and the correction CFL numbers are shown in **Figures 3.14** and **3.15** for M = 0.2 and in **Figures 3.16** and **3.17** for M = 10.

What are some of the general features? The most obvious one is that the correction CFL is typically of order unity whilst the discrete CFL is an order of magnitude or more greater. If a CFL limit of unity must be satisfied for an accurate solution, then we begin to understand the effectiveness of streamline simulation: our time step sizes can be an order of magnitude or more greater than conventional simulation. This is consistent with the literature reports of 10-100 fold improvements in simulation run times by streamline simulators compared to conventional finite difference simulation.[3]

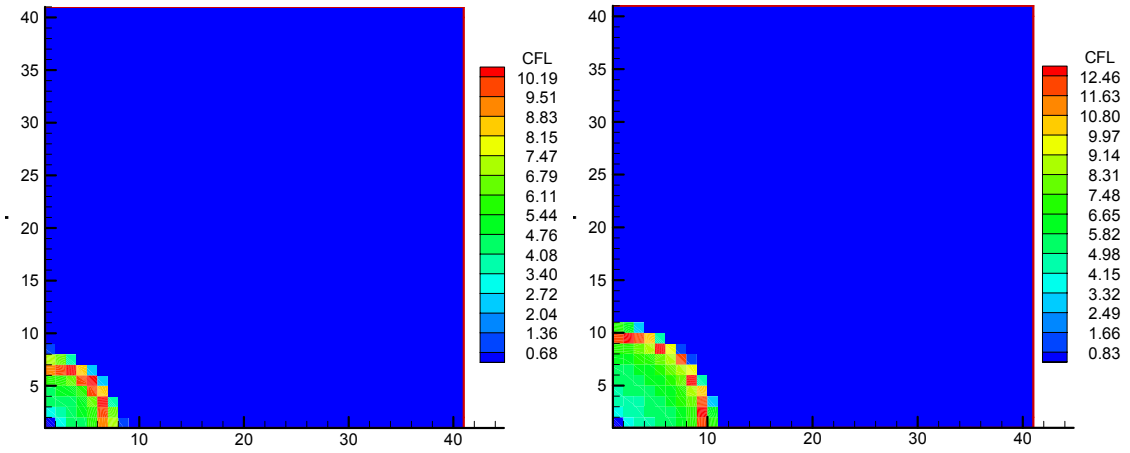

Δt = 10 days CFL_{MAX}=10.871 Δt = 20 days CFL_{MAX}=13.293

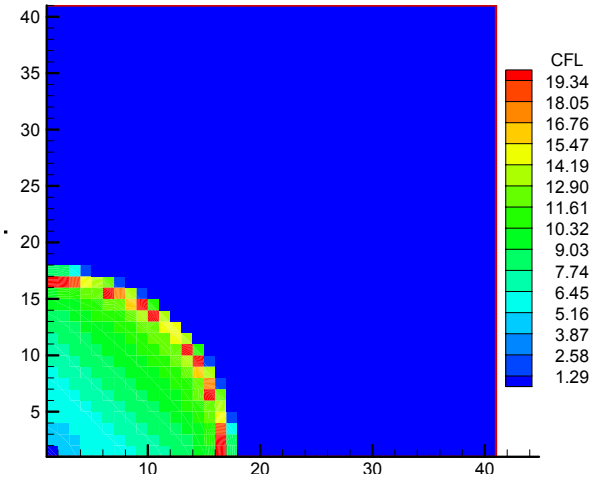

Δt = 60 days CFL_{MAX}=20.633

Figure 3.10 The spatial distribution of discrete CFL numbers for various pressure timesteps: M=0.2 homogeneous case

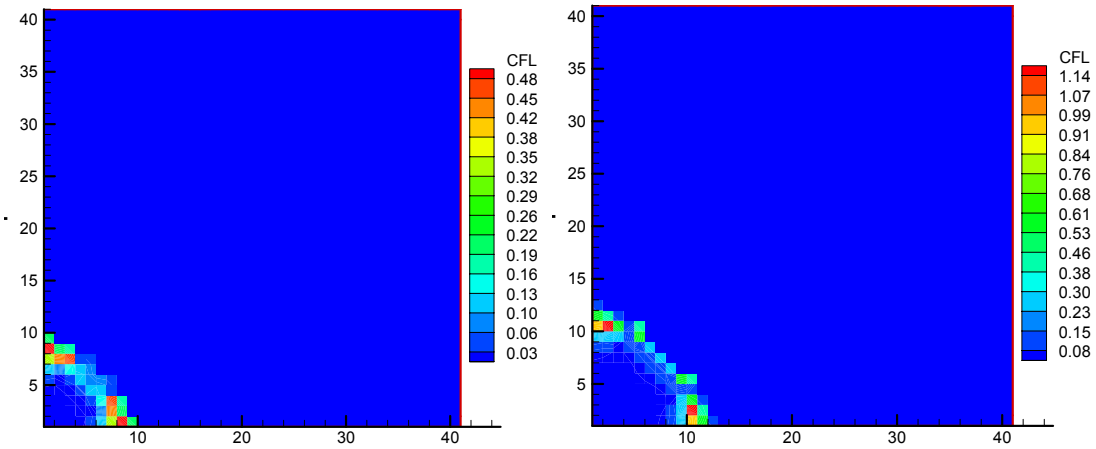

Δt = 10 days CFL_{MAX} =0.513 Δt = 20 days CFL_{MAX} =1.217

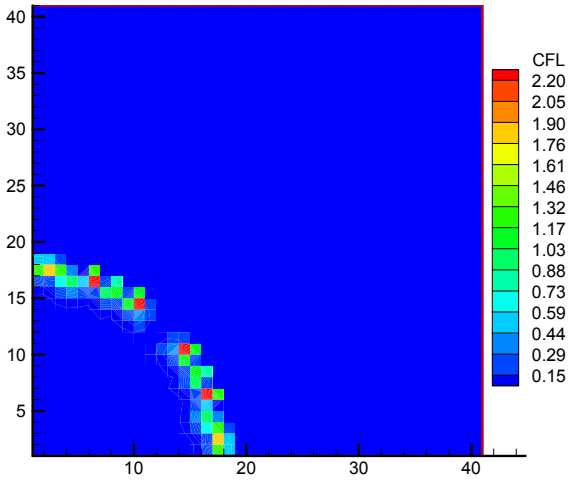

Δt = 60 days CFL_{MAX} =2.343

Figure 3.11 The spatial distribution of correction CFL numbers for various pressure timesteps: M=0.2 homogeneous case

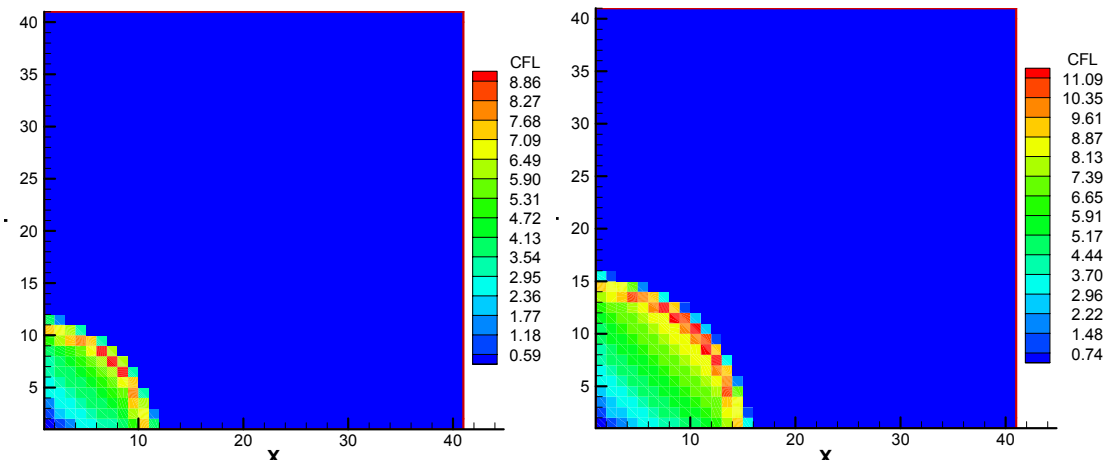

$\Delta t = 10$ days $CFL_{MAX} = 9.447$ $\Delta t = 20$ days $CFL_{MAX} = 11.827$

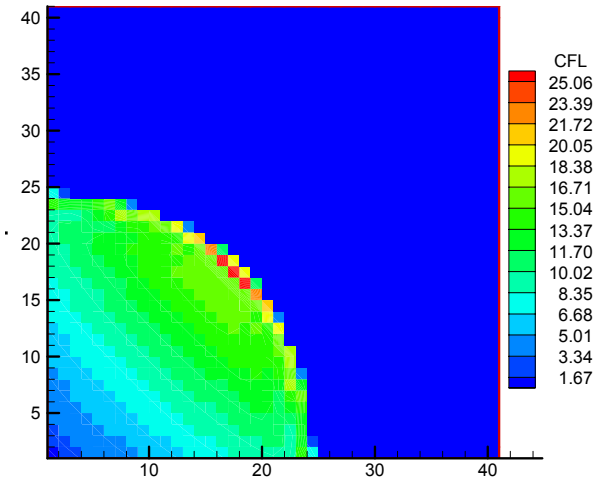

$\Delta t = 60$ days $CFL_{MAX} = 26.732$

Figure 3.12 The spatial distribution of discrete CFL numbers for various pressure timesteps: M=10 homogeneous case

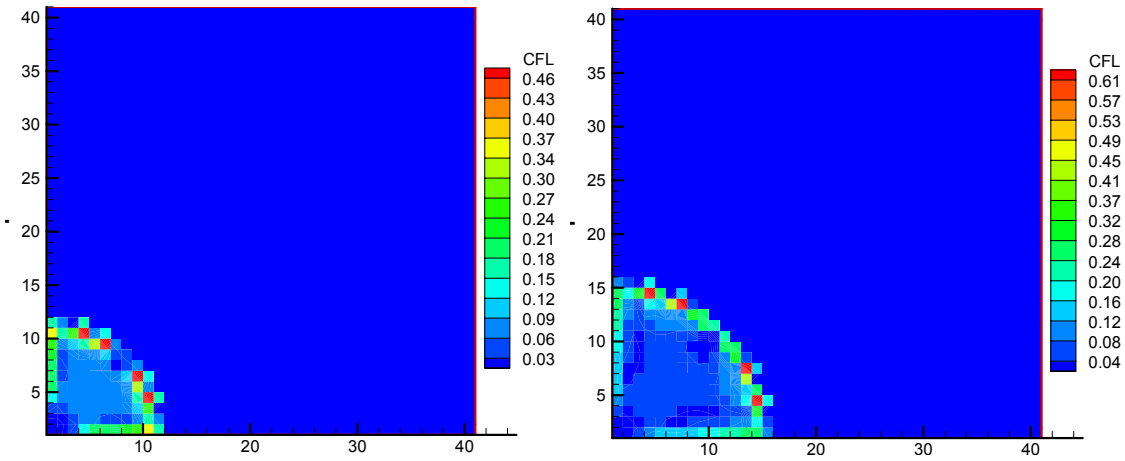

$\Delta t = 10$ days $CFL_{MAX} = 0.488$ $\Delta t = 20$ days $CFL_{MAX} = 0.649$

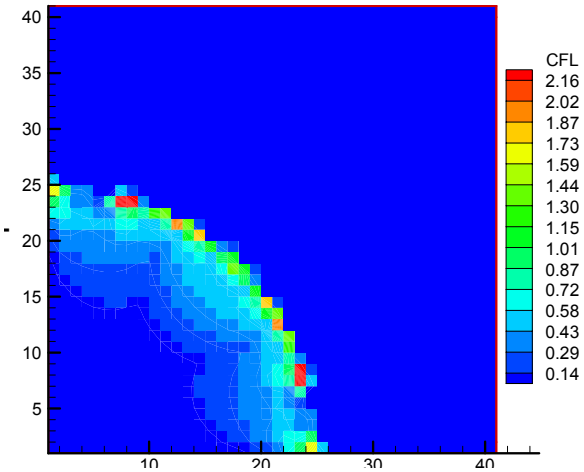

$\Delta t = 60$ days $CFL_{MAX} = 2.307$

Figure 3.13 The spatial distribution of correction CFL numbers for various pressure timesteps: M=10 homogeneous case

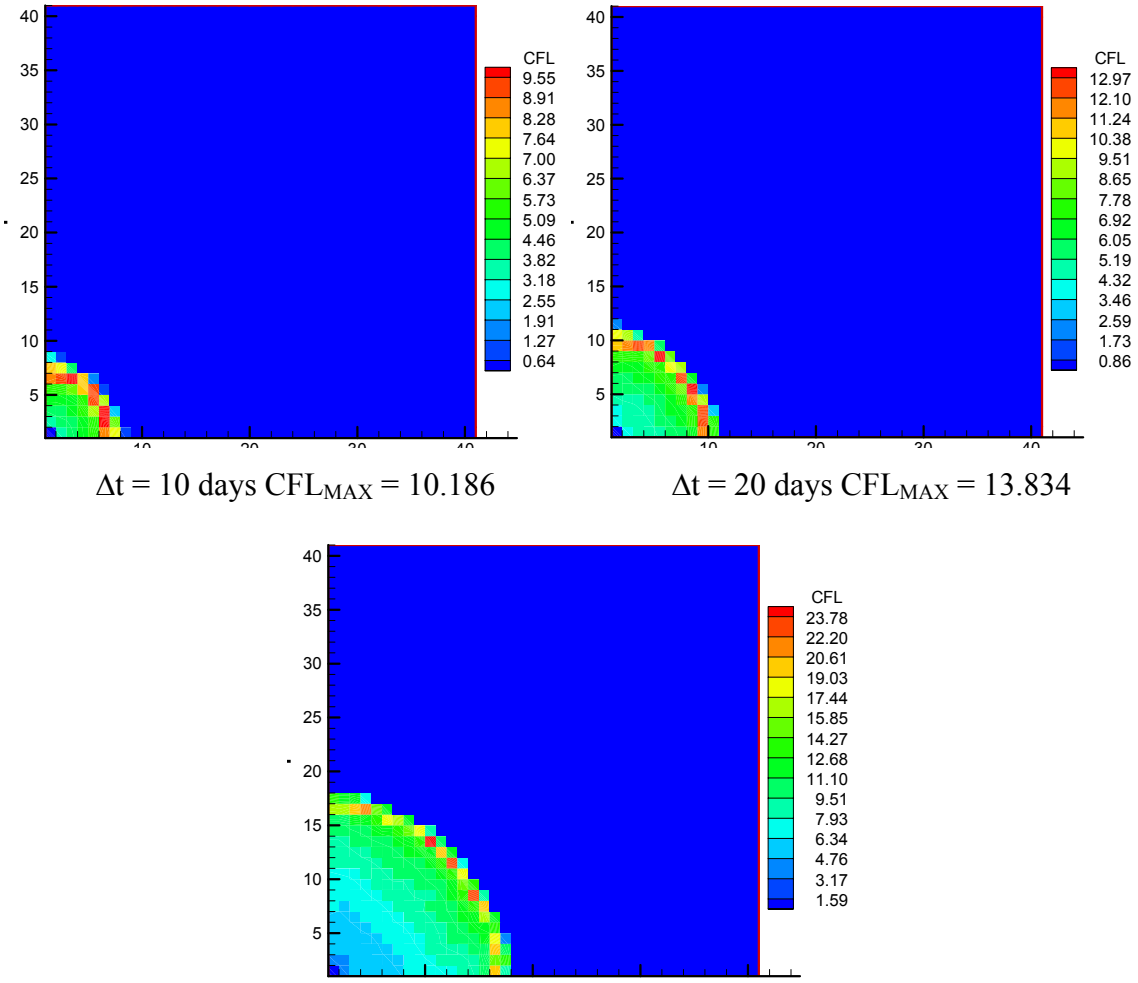

$\Delta t = 10$ days $CFL_{MAX} = 10.186$

$\Delta t = 20$ days $CFL_{MAX} = 13.834$

$\Delta t = 60$ days $CFL_{MAX} = 26.367$

Figure 3.14 The spatial distribution of discrete CFL numbers for various pressure timesteps: M=0.2 heterogeneous case

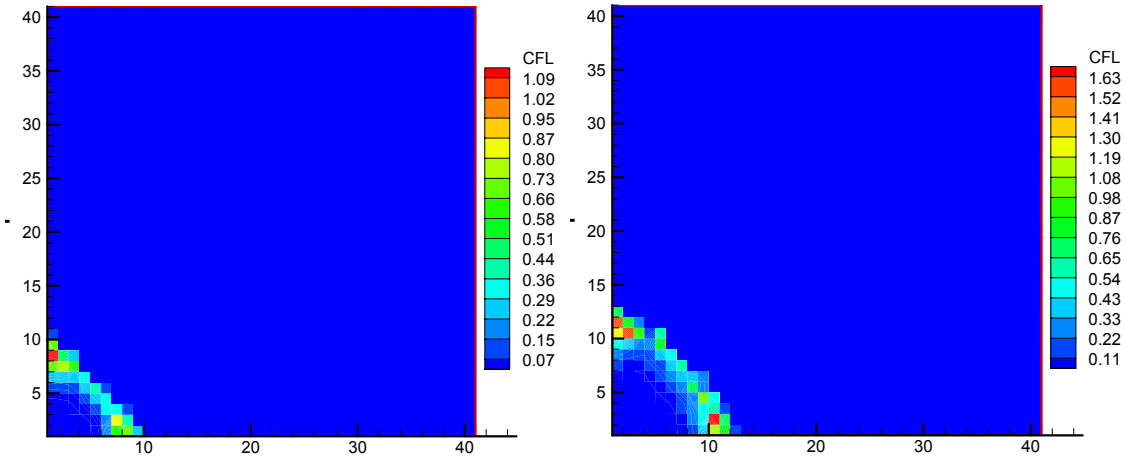

Δt = 10 days CFL_{MAX} = 1.166 Δt = 20 days CFL_{MAX} =1.735

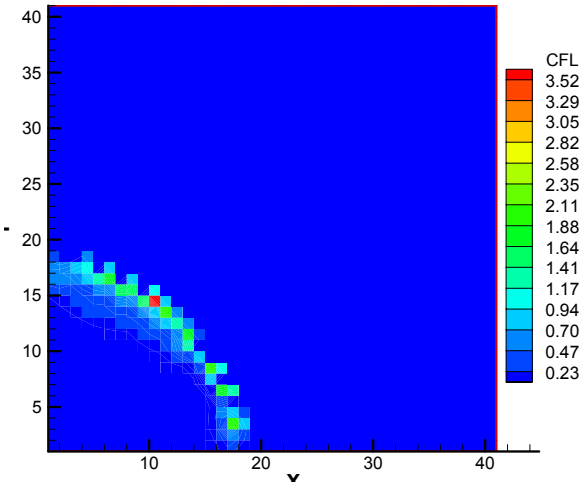

Δt = 60 days CFL_{MAX} = 3.755

Figure 3.15 The spatial distribution of correction CFL numbers for various pressure timesteps: M=0.2 heterogeneous case

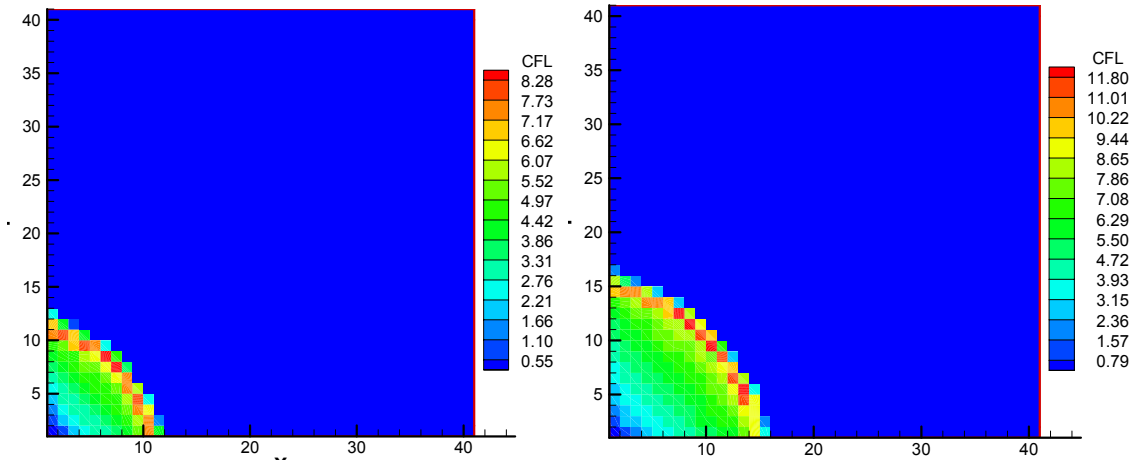

$\Delta t = 10$ days $CFL_{MAX} = 8.830$ $\Delta t = 20$ days $CFL_{MAX} = 12.582$

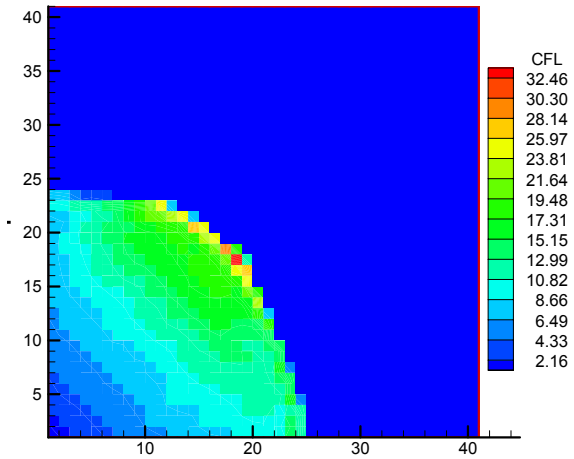

$\Delta t = 60$ days $CFL_{MAX} = 34.628$

Figure 3.16 The spatial distribution of discrete CFL numbers for various pressure timesteps: M=10 heterogeneous case

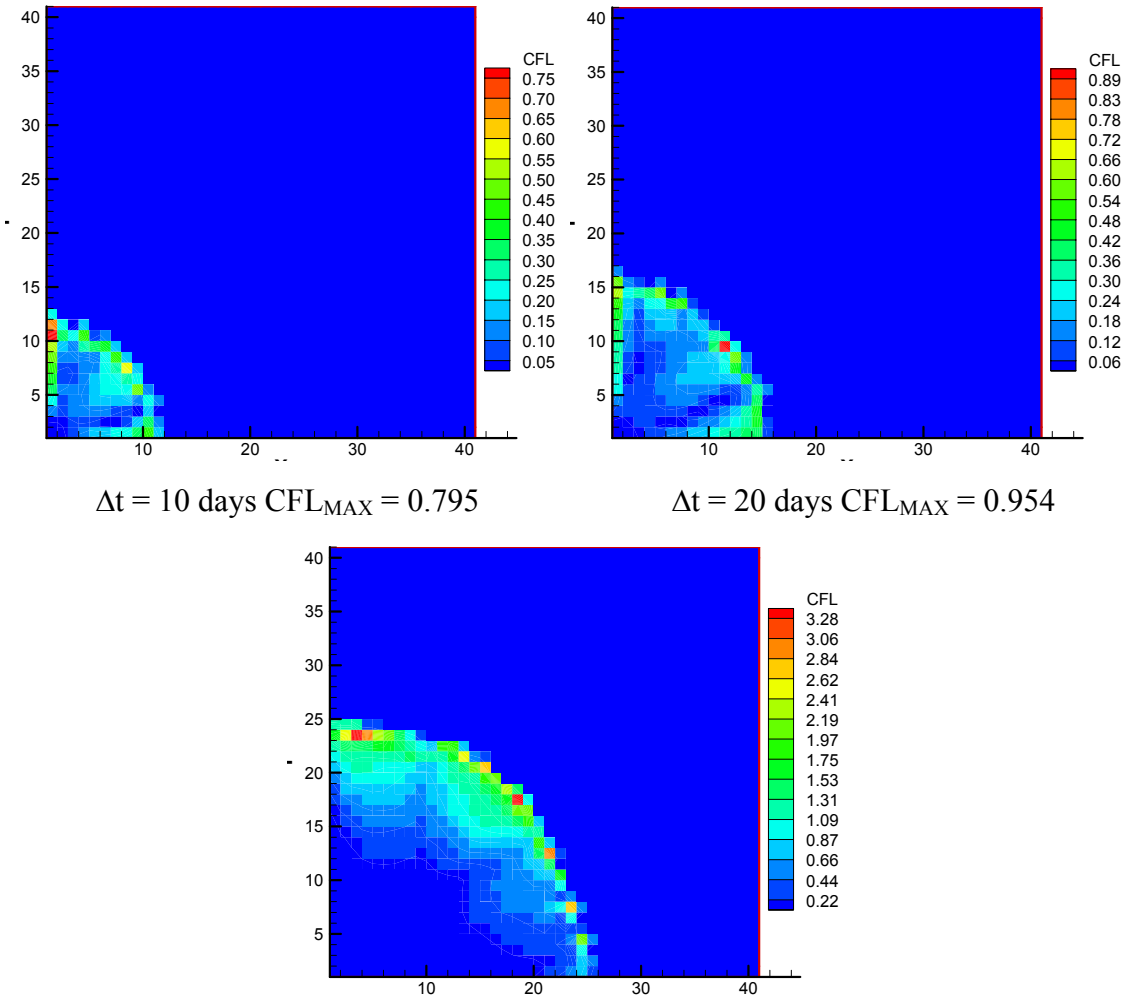

$\Delta t = 10$ days $CFL_{MAX} = 0.795$

$\Delta t = 20$ days $CFL_{MAX} = 0.954$

$\Delta t = 60$ days $CFL_{MAX} = 3.498$

Figure 3.17 The spatial distribution of correction CFL numbers for various pressure timesteps: M=10 heterogeneous case

A second observation is that the value of the correction CFL relative to unity does describe the numerical stability of the solution. This is made obvious in the summary report of **Table 3.1.**, where we have now included results corresponding to four mobility ratios, $M = 0.2$, 0.5, 0.9 and 10. All unstable solutions identified in **Figure 3.2 to Figure 3.9** are shaded in. Clearly, $CFL = 1$ is the limit of stability.

Table 3.1. Maximum correction CFL

(Unstable results are shaded)

		Time step (days)		
Correction CFL		10	20	60
Homogeneous	M=0.2	0.513	1.218	2.343
	M=0.5	0.567	0.716	1.385
	M=0.9	0.298	0.468	1.47
	M=10	0.488	0.649	2.306
Heterogeneous	M=0.2	1.166	1.73	3.755
	M=0.5	0.884	1.362	2.679
	M=0.9	0.689	1.006	1.794
	M=10	0.705	0.954	1.59

A third observation involves the difference in the spatial pattern between the discrete and correction CFL's. Both CFL constructions take on a maximum at the flood front because of the ∇f_w term, but of course, there is also a fractional flow gradient throughout the profile. However, the correction CFL is fairly sharply limited to the flood front. In this location, both $(\vec{u}-\vec{u}_0)$ and ∇f_w are relatively large. However, in the bulk of the profile, $(\vec{u}-\vec{u}_0)$ and ∇f_w tend to be orthogonal, e.g., the velocity corrections correspond to transverse flow.

3.3 Water Saturation distribution Analysis

Figures 3.18 and **3.19** examine the waterflood results (M = 0.2 and 10) for the homogeneous permeability field in more detail. Now we plot out the water saturation distribution after 0.4 PVI for various time steps. For comparison purposes, the results from Eclipse are also shown in the plots.

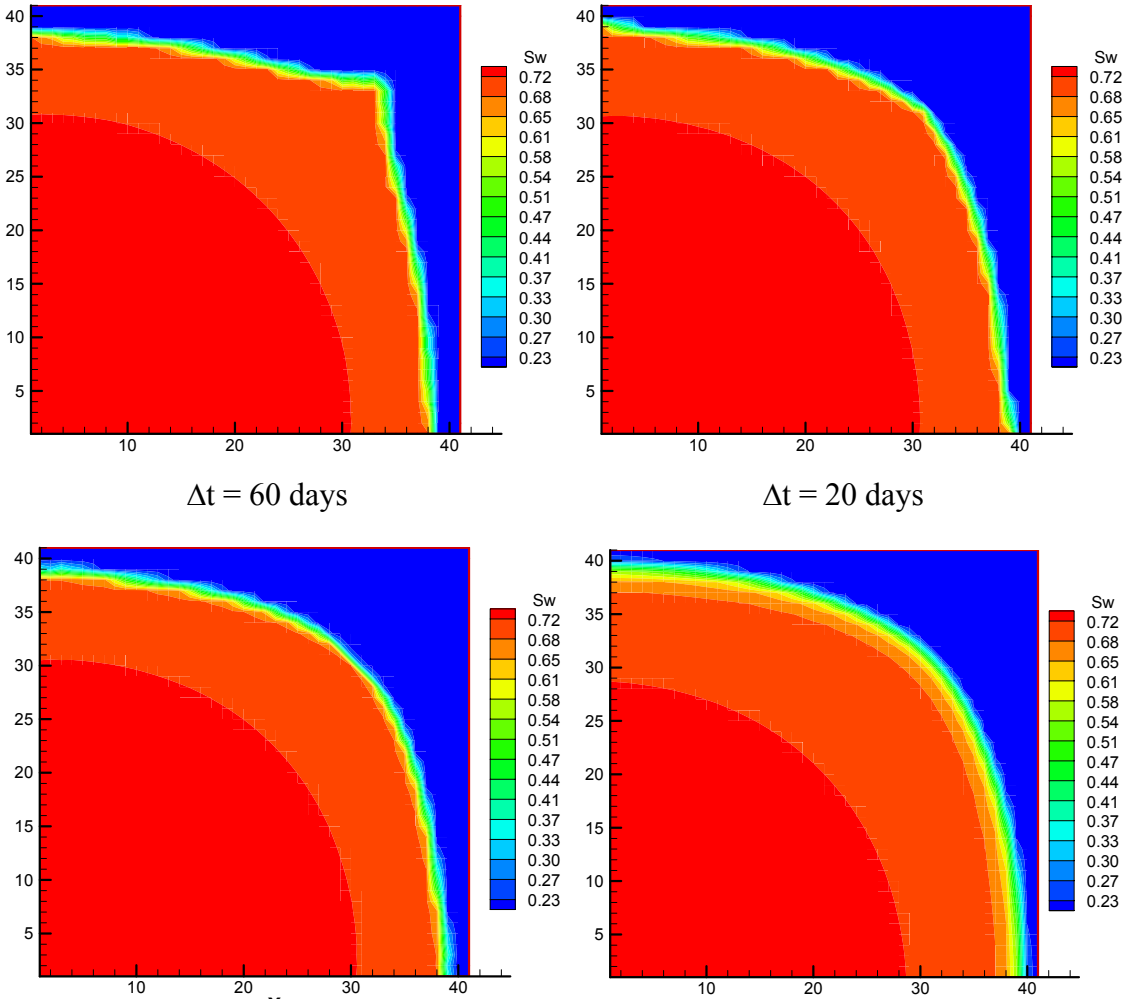

Δt = 60 days

Δt = 20 days

Δt = 10 days

ECLIPSE

Figures 3.18 Saturation profile of 0.4 PVI for various pressure timesteps: M=0.2 homogeneous case

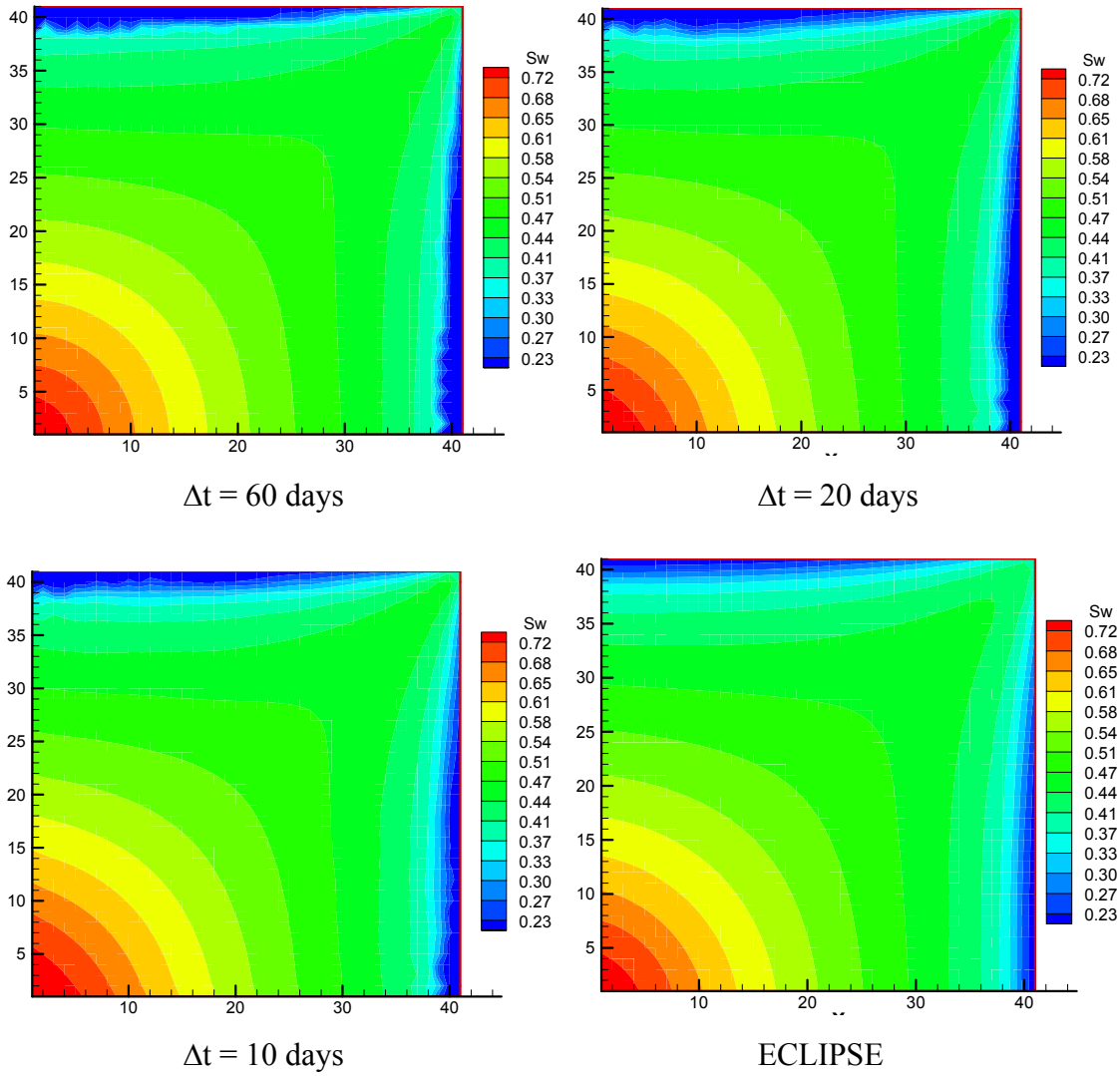

Figures 3.19 Saturation profile of 0.4 PVI for various pressure timesteps: M=10 homogeneous case

We see that the larger time steps do not allow the velocities within the simulation sufficient flexibility to respond to the waterflood mobilities. However, as the time step size decreases, the saturation plots become essentially identical to those calculated with Eclipse. Similar observations can be made for the heterogeneous permeability field and the results for this case are shown in **Figures 3.20** and **3.21**.

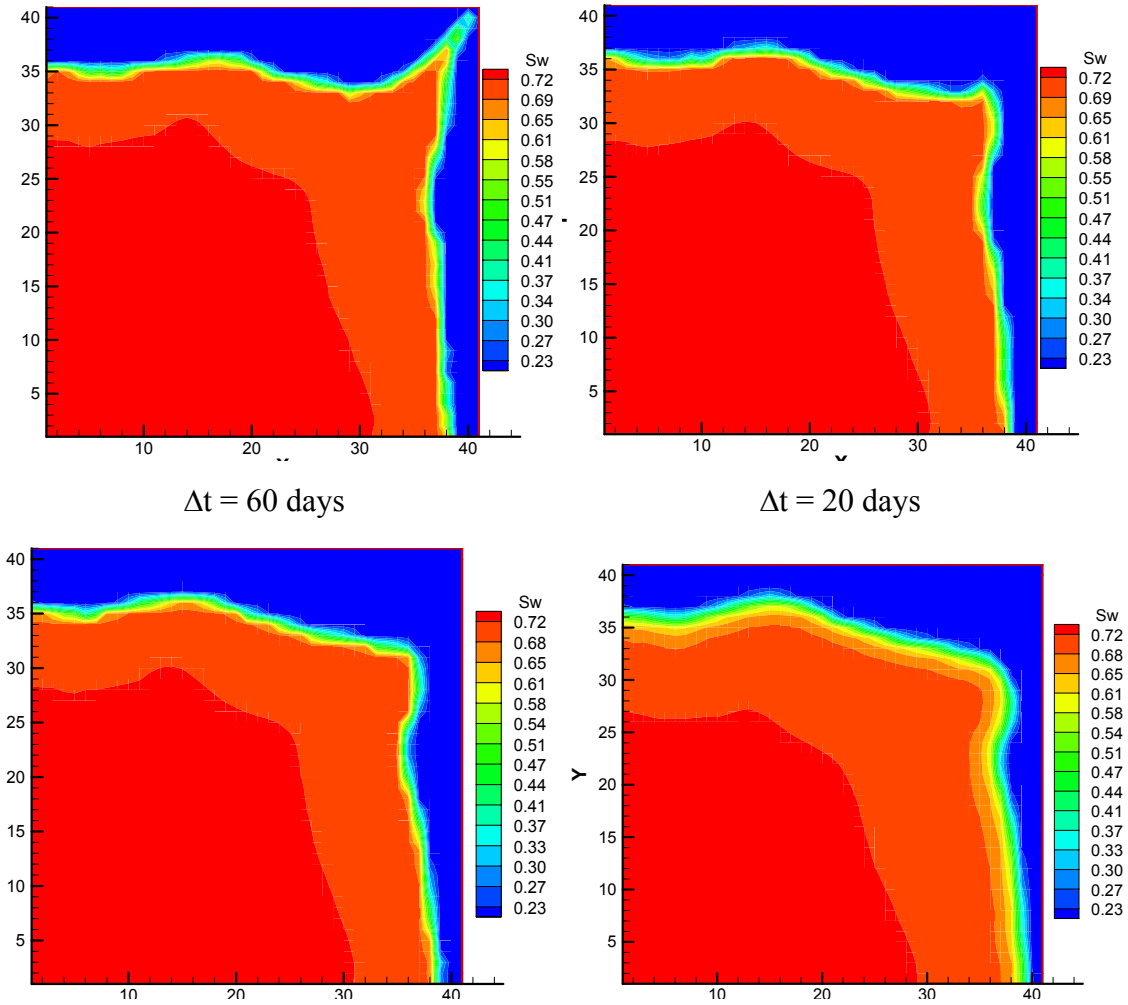

Δt = 60 days

Δt = 20 days

Δt = 10 days

ECLIPSE

Figures 3.20 Saturation profile of 0.4 PVI for various pressure timesteps: M=0.2 heterogeneous case

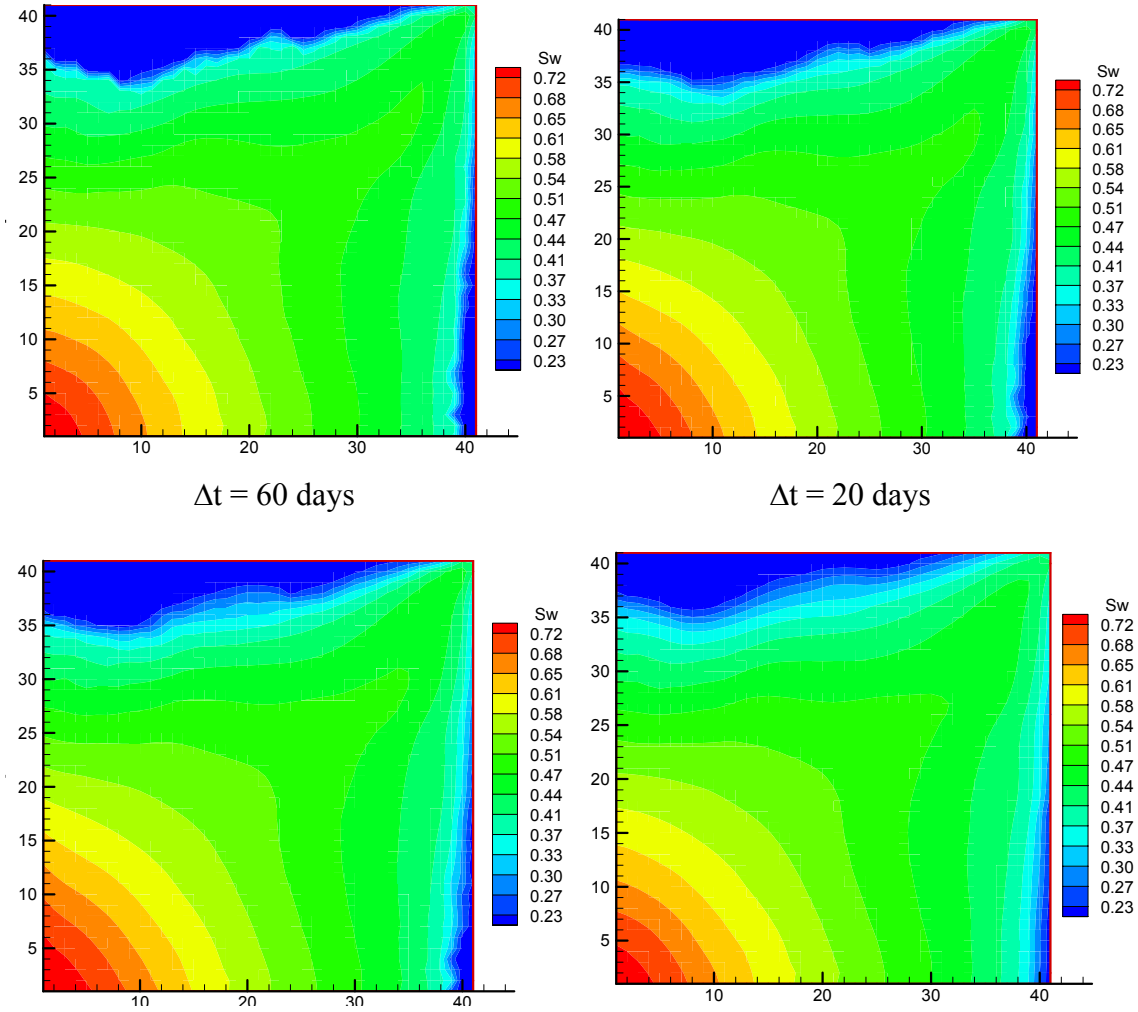

Figures 3.21 Saturation profile of 0.4 PVI for various pressure timesteps: M=10 heterogeneous case

3.4 Optimal Timestep Calculation Using Correction CFL

A final application of the use of the correction CFL is shown in **Figure 3.22**. If for a given time step size the correction CFL is equal to 0.5, then we can probably safely double the time step size. Or, if the correction CFL is equal to 2.0, then we need to half the time step size. In other words, dividing the time step size by the correction CFL

gives an estimate of the optimal time step size. **Figure 3.22** is the plot of optimal versus actual time steps, with a diagonal line for a reference. Any simulation above the diagonal is numerically stable and the others are not. There clearly is room for optimization here in terms of time step selection, if one chose to implement such an algorithm. Thus, the correction CFL lays the foundation for a potential adaptive time step control scheme for streamline simulation.

As an aside, in the diverging flow geometry of the quarter five spot, in which earlier times have faster velocities, one would not expect that a simple linear estimate of optimal time is especially accurate. In fact, it is not. However, the biases are in the direction one would expect.

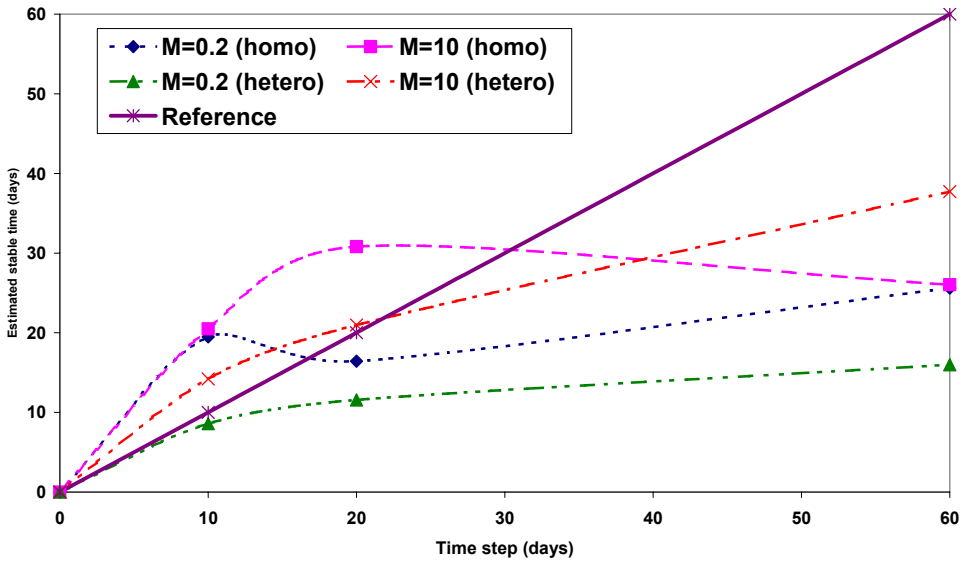

Figure 3.22 Actual timestep vs. estimated stability limit for ¼ five spot example

3.5 Saturation Corrections and Numerical Accuracy

Let's now return to the question of the saturation corrections, **Eq.(2.15)**. In **Figures 3.23** and **3.24** we plot out the water cuts for the end member examples: M = 0.2 and 10,

homogeneous and heterogeneous. Some of this data was presented in **Figure 3.2**, but now we include the solutions both with and without the saturation corrections. Interestingly, we see very little impact of the corrections.

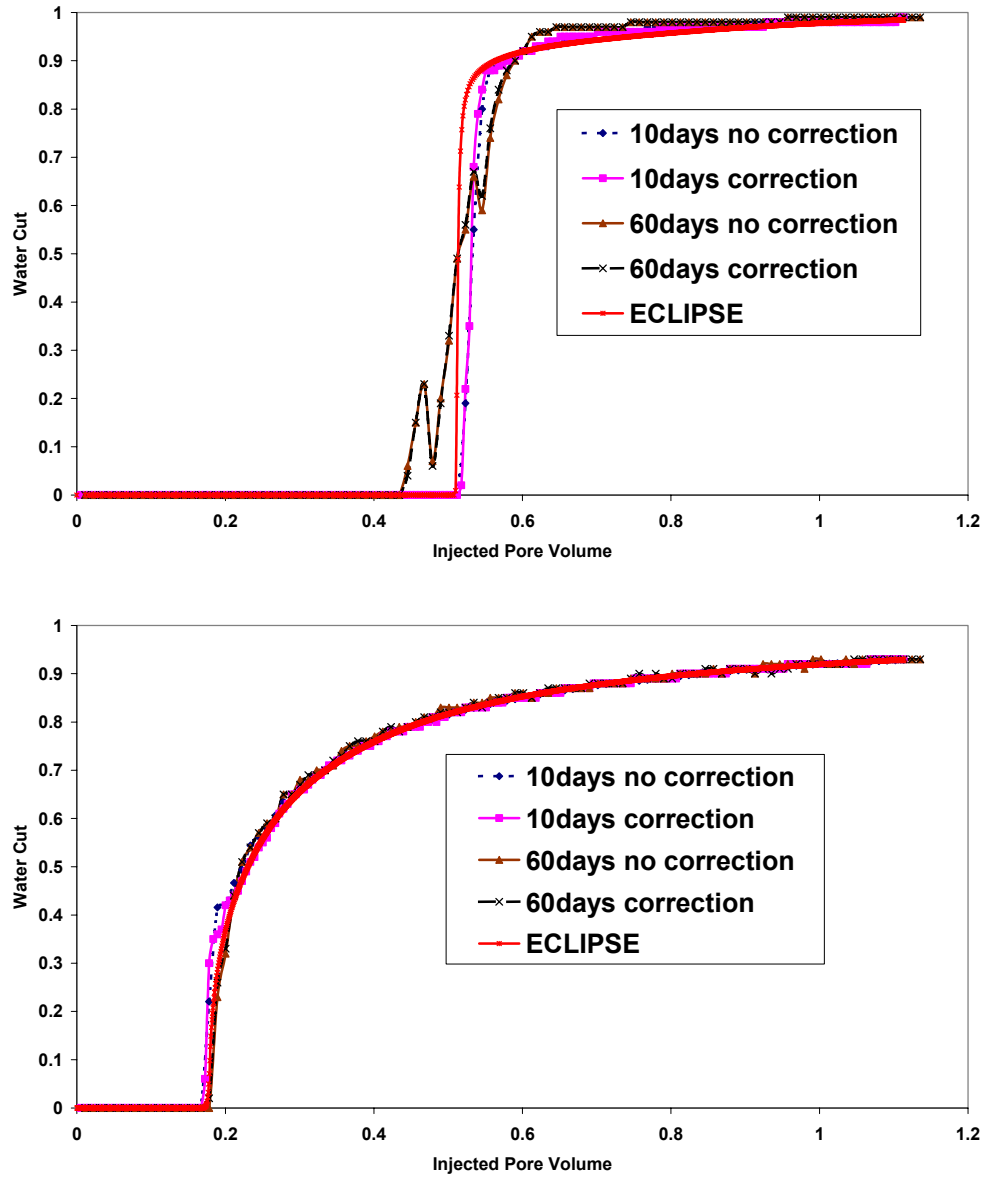

Figure 3.23 Impact of saturation correction for M=0.2 and M=10: homogeneous case

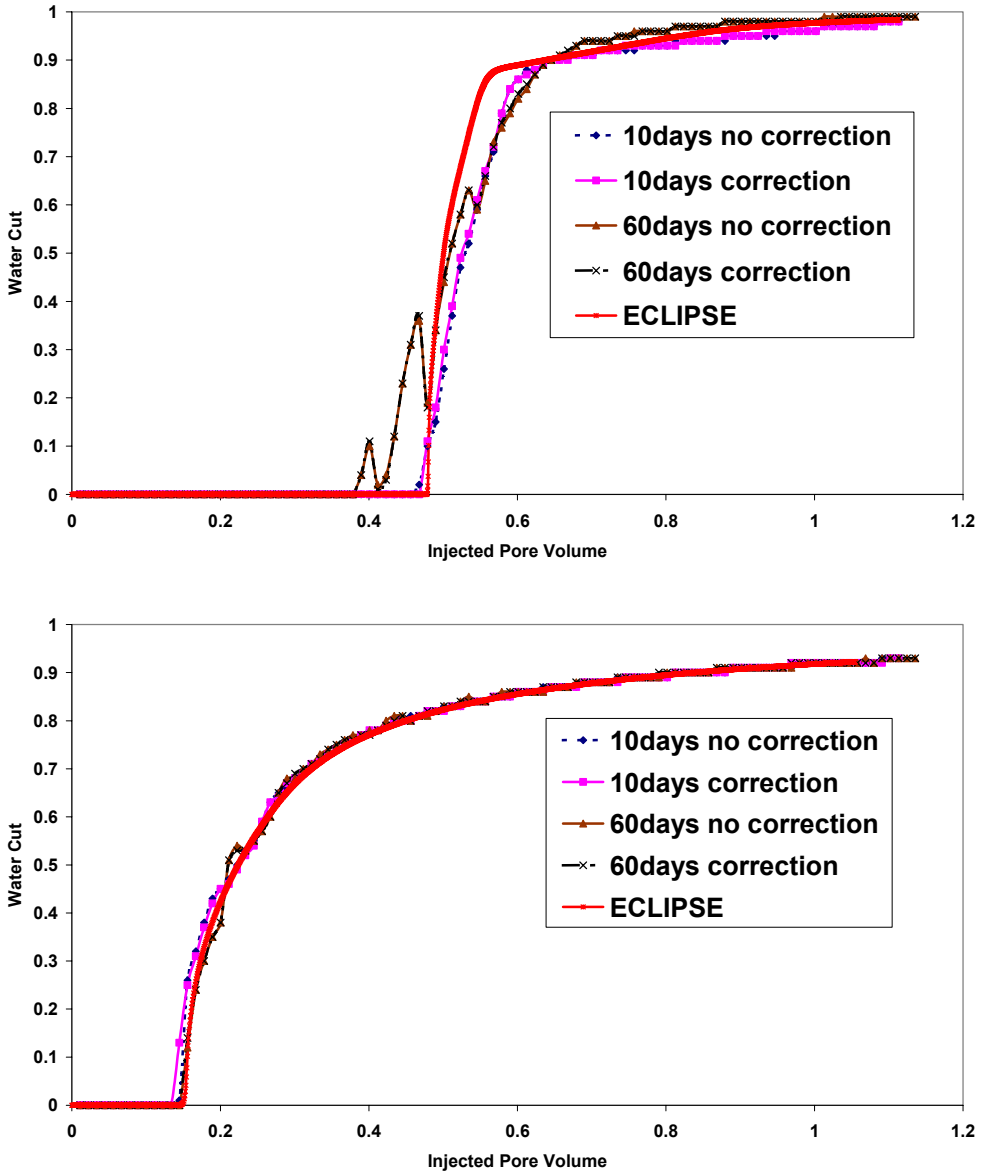

Figure 3.24 Impact of saturation correction for M=0.2 and M=10: heterogeneous case

In **Figures 3.25** and **3.26** we plot the saturation corrections areally, for these cases, for a 60 day time step and a smaller numerically stable time step. For M = 0.2, this corresponds to a time step size of 5 days. Maximum saturation corrections are included in the legend.

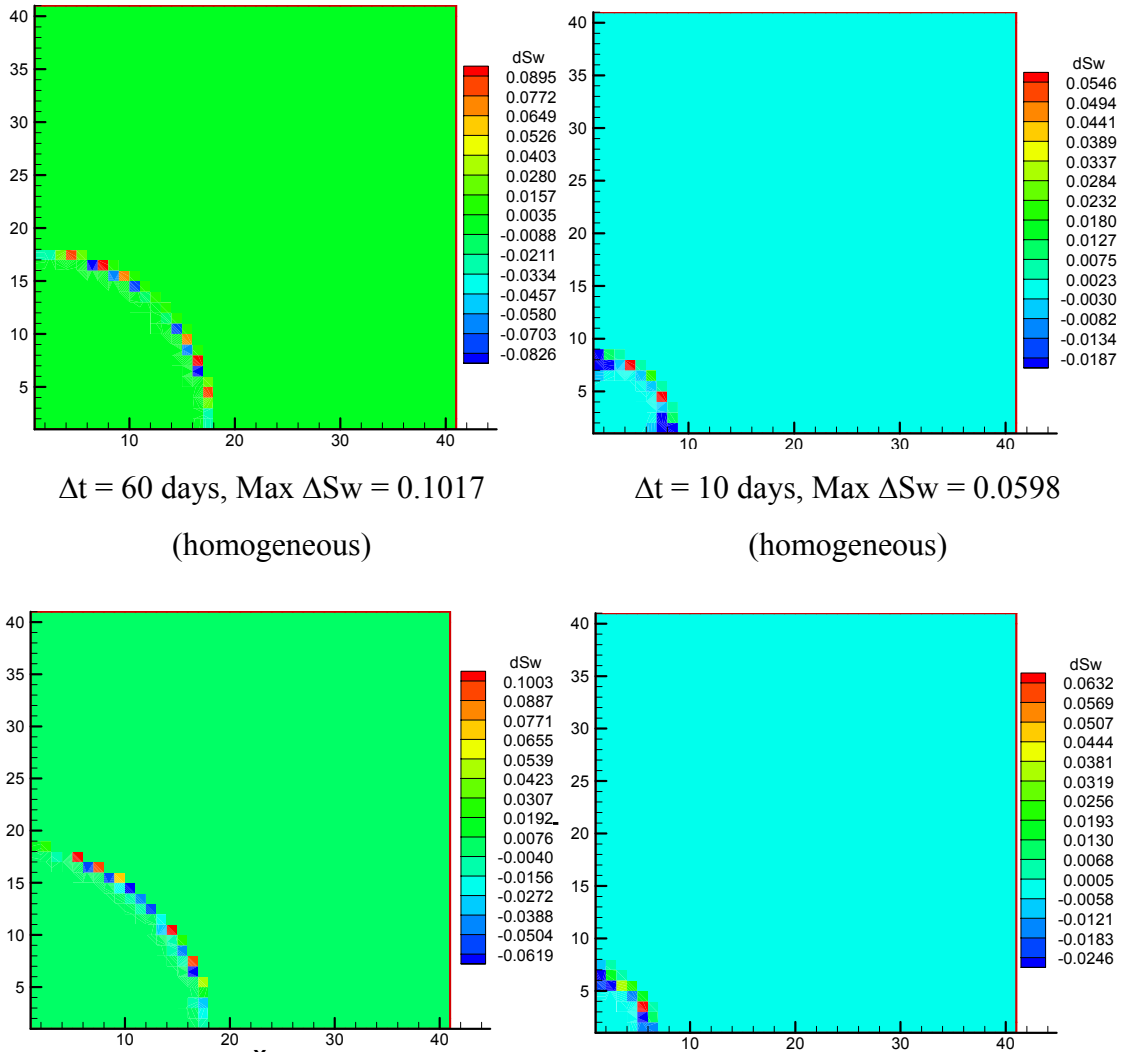

Δt = 60 days, Max ΔSw = 0.1017 (homogeneous)

Δt = 10 days, Max ΔSw = 0.0598 (homogeneous)

Δt = 60 days, Max ΔSw = 0.1183 (heterogeneous)

Δt = 5 days, Max ΔSw = 0.0694 (heterogeneous)

Figure 3.25 Saturation correction value profile for M=0.2

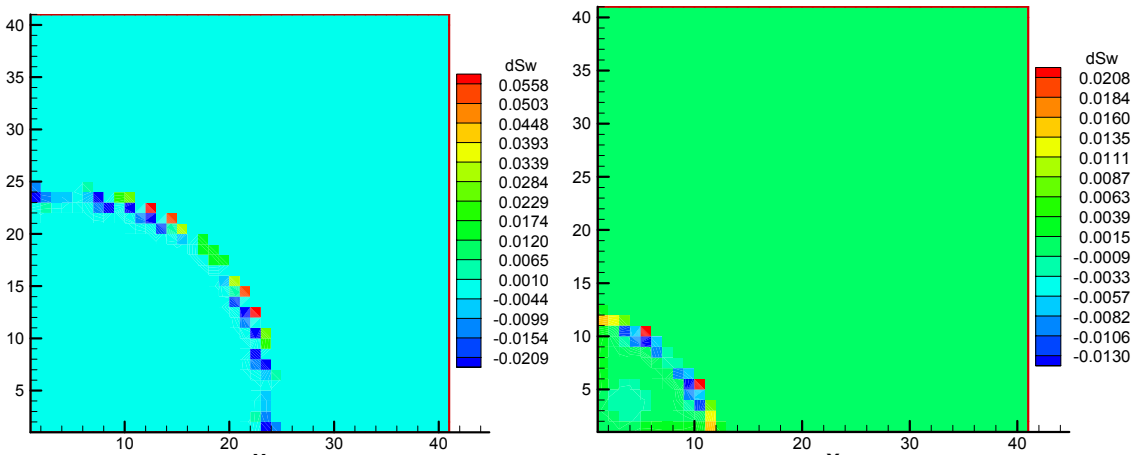

Δt = 60 days, Max ΔSw = 0.0612 (homogeneous)

Δt = 10 days, Max ΔSw = 0.0231 (homogeneous)

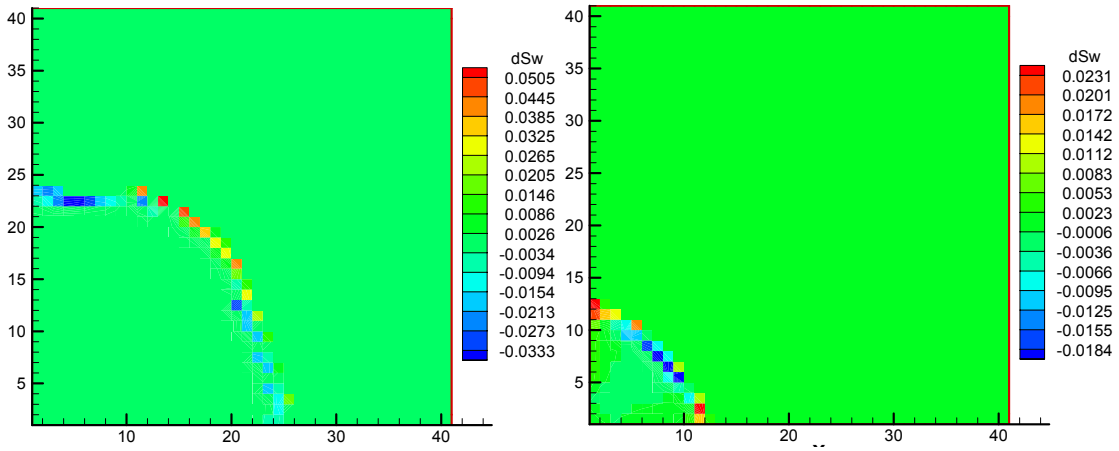

Δt = 60 days, Max ΔSw = 0.0564 (heterogeneous)

Δt = 10 days, Max ΔSw = 0.0260 (heterogeneous)

Figure 3.26 Saturation correction value profile for M=10

Although individual cell saturation changes may appear large for the unstable 60 day simulation runs, for the converged case, the corrections seem to be small. A summary of this information for all the cases, after the first time step, is shown in **Table 3.2.**. Again,

the numerically unstable cases are shaded. We find that generally when the saturation corrections are large that the solutions are numerically unstable, while they are small for the stable cases. We may be in the very interesting situation that the primary utility of **Eq.(2.15)** is for numerical stability and not for saturation corrections. In other words, it may never actually need to be solved, but it is central to understanding the numerical stability of **Eq.(2.13)** and the choice of a stable time step for pressure updates.

Table 3.2. Maximum saturation correction

(Unstable results are shaded)

		Time step (days)		
ΔS_w Max		10	20	60
Homogeneous	M=0.2	0.0598	0.0419	0.1017
	M=0.5	0.022	0.0894	0.0838
	M=0.9	0.0147	0.0395	0.0765
	M=10	0.0231	0.0209	0.0612
Heterogeneous	M=0.2	0.0472	0.0914	0.1183
	M=0.5	0.0742	0.0757	0.0949
	M=0.9	0.0352	0.0309	0.0840
	M=10	0.0260	0.0372	0.0564

CHAPTER IV
CONCLUDING REMARKS

We have provided an analysis for the numerical stability of streamline simulation. This analysis supports our physical intuition and industry experience with streamline simulations. For the first time, it also supplies a quantitative means of assessing the quality of the approximation. We have restricted our attention to the simplest of waterflood equations to demonstrate our approach. However, now that the approach has been defined, it is fairly clear how to extend the results to more complex equations and processes. The requirement for increased rigor in streamline simulation is becoming even more apparent as we move away from "simple" waterflood to compositional simulation. We can no longer expect that simple screening studies or engineering insight will be sufficient to understand whether these calculations are mechanistic or are totally fallacious.

Some specific conclusions from this study can be summarized as follows:

- We have derived a pair of equations for streamline simulation that are equivalent to the usual full set of finite difference multiphase flow equations. One equation is recognized as that usually solved by streamline simulators. The second equation includes all of the unsteady state velocity and transverse flux terms neglected by the first equation.
- Of these two equations, the first only includes transport along streamlines, and can be solved using the techniques in any of the commercial streamline simulators. At each time step this involves re-sampling saturations from cells to lines, solving the flow equations along the lines, and then averaging or sampling saturations back to the cells.
- The second equation is simple to implement on a cell basis, and may be treated as a corrector step at the end of each streamline time step. In form, the second equation is

identical to that of our conventional finite difference formulations, except that phase velocity is replaced with a correction velocity.

- We have defined a discrete CFL number based on the corrector equations. We have shown that even when the corrections are small, that the numerical stability of the streamline approximation is the limit of stability of the correction equation.

  We can now think of a synthesis of streamline and conventional simulation, with the speed of the streamline methods merged with the rigor of the conventional finite difference approach.

And also we propose future work as follows:

1. Evaluation of Instability Criteria

   We have found the instability of the watercut response manually in case of the correction CFL number is greater than unity. Since the watercut response from quarter five spot cases give us the monotonic curve with time, oscillations found in watercut response will tell us instability clearly. However when we have changing well rates and different well patterns the monotonic characteristics might be lost or hard to detect. And also those changes of well conditions might affect the correction CFL number at the same time. Therefore to overcome these restrictions and difficulties we need to find a more rigorous the instability criteria.

2. Applications for more complex fluids

   As we mentioned before, our approach has been defined in simple waterflood case. It is fairly clear how to extend the results to more complex equations and processes. We can implement capillarity, compressibility, gravity and so on using the saturation correction equation and also includes all of the unsteady state velocity and transverse flux terms neglected by the conventional streamline

equation. We need to show the applications for those cases and evaluate the validity of a discrete CFL formulation for the streamline simulation.

NOMENCLATURE

CFL = Courant-Fredrich-Levy

f_w = fractional water saturation

k = permeability

k_{rp} = relative permeability, phase *P*=Oil, Water

M = mobility ratio

$\vec{n}_f$ = cell face area vecotr (normal)

$\hat{n}$ = cell face area vector (unit normal)

P = pressure

PV = cell pore volume

S_w = water saturation

S_{orw} = residual oil saturation

S_{wirr} = irreducible water saturation

t = time

t_1, t_2 = time split times

$\vec{u}$ = total Darcy velocity

$\vec{u}_0$ = initial total Darcy velocity

Δt = time step size

Δx = cell size (one-dimensional)

τ = time of flight

ϕ = porosity

ψ, χ = bi-streamfunctions

μ_p = viscosity, phase P=Oil, Water

λ_t = total mobility

REFERENCES

1. Bratvedt, F., Bratvedt, K., Buchholz, C. F., Gimse, T., Holden, H., Holden, L. and Risebro, N. H., "FRONTLINE and FRONTSIM. Two Full Scale, Two-Phase, Black Oil Reservoir Simulators Based on Front Tracking," *Surv. Math. Ind.*, **3**, 185 (1993).
2. Datta-Gupta, A. and King, M.J.: "A Semianalytic Approach to Tracer Flow Modeling in Heterogeneous Permeable Media," *Adv. in Water Resources,* **18** (1), 9 (1995).
3. King, M. J. and Datta-Gupta, A., "Streamline Simulation: A Current Perspective," *In Situ*, **22**(1), 91-140, 1998.
4. Bratvedt, F., Gimse, T. and Tegnander, C., "Streamline Computations for Porous Media Flow Including Gravity," *Transport in Porous Media*, **25**, 63 (1996).
5. Crane, M. J. and Blunt, M. J., "Streamline-based Simulation of Solute Transport," *Water Resour. Res.*, **35**(10), 3061-3078, 1999.
6. Behrens, R. A., Jones, R. C. and Emanuel, A. S., "Implementation of a Streamline Method for Flow Simulation of Large Fields," *Journal of Canadian Petroleum Technology*, Special Edition, **38** (13), 1999.
7. Ponting, D. K., "Hybrid Streamline Methods," paper SPE 39756 presented at the 1998 Asia Pacific Conference on Integrated Modeling, Kuala Lumpur, Malaysia, 23-24 March, 1998.
8. Jessen, K. and Orr, F. M., "Compositional Streamline Simulation," paper SPE 77379 Presented at the SPE Annual Technical Conference and Exhibition, San Antonio, TX, Sept. 29-Oct. 2, 2002.
9. Rodriguez, G. P. Segura, M. K., and Mustieles Moreno, F. J., "Streamline Methodology Using an Efficient Operator Splitting for Accurate Modeling of Capillarity and Gravity Effects," paper SPE 79693 presented at the SPE Reservoir Simulation Symposium, Houston, TX, 2-5 February, 2003.

10. Coats, K. H., “IMPES Stability: The CFL Limit,” paper SPE 66345 presented at the SPE Reservoir Simulation Symposium, Houston, TX, 11-14 February, 2001.
11. Datta-Gupta, A., Lake, L. W., Pope, G. A. and King, M. J., “A Type-Curve Approach to Analyzing Two-Well Tracer Tests,” paper SPE 24139 Presented at the SPE/DOE Symposium on EOR, Tulsa, OK (1992). Also, *SPE Form. Eval*., **10**, 40 (1995).
12. King, M. J., Blunt, M., Mansfield, M. and Christie, M. A., “Rapid Evaluation of the Impact of Heterogeneity on Miscible Gas Injection,” paper SPE 26079 Presented at the SPE Western Regional Meeting (1993). Also in *New Developments in Improved Oil Recovery*, H. J. De Haan (ed.), Geological Society Special Publication 84, Bath, UK (1995).
13. Lake, L. W., *Enhanced Oil Recovery*, Prentice Hall, Englewood Cliffs, NJ (1989).
14. Aziz, K. and Settari, A., *Petroleum Reservoir Simulation*, Applied Science Publishers, Essex, England (1979).
15. Kulkarni, K. N., Datta-Gupta, A. and Vasco, D. W., "A Streamline Approach to Integrating Transient Pressure Data into High Resolution Reservoir Models," *SPE Journal*, **6**(3), September 2001.
16. Bear, J., *Dynamics of Fluid in Porous Media*, Dover Publications, New York (1973).
17. Bratvedt, F., Bratvedt, K., Buchholz, C. F., Holden, L., Holden, H. and Risebro, N. H., “A New Front Tracking Method for Reservoir Simulation,” *SPE Reser. Eng*., **7**, 107 (1992).
18. Trangenstein, J. A., “Numerical Analysis of Reservoir Fluid Flow, Multiphase Flow in Porous Media: Mechanics, Mathematics and Numerics,” *Lecture Notes in Engineering*, (34), p87-246, Springer Verlag, NY (1988).
19. Spivak, A. and Coats, K. H., “Numerical Simulation of Coning Using Implicit Production Terms,“ *SPE Journal*, 257-267, September (1970).

20. Osako, I., Datta-Gupta, A. and King, M. J., “Time Step Selection During Streamline Simulation via Transverse Flux Correction,” paper SPE 79688 presented at the SPE Reservoir Simulation Symposium, Houston, TX, February 3-5, 2003.
21. Schlumberger Geoquest, *ECLIPSE 100* Reference Manual, Schlumberger, Houston, TX (2000).

VITA

Ichiro Osako received his B.Eng. degree in environmental and mineral resources engineering from Waseda University, Tokyo, Japan, in March 2001.

His current address: Texas A&M University
3116 TAMU
401 Richardson Building
College Station, Texas
USA

His permanent address: 339 Asano
Munakata, Fukuoka
Japan, 811-3415